Sustainable Chemistry for the Environment 3 (2023) 100034

Contents lists available at ScienceDirect

Sustainable Chemistry for the Environment

journal homepage: www.editorialmanager.com/scenv

Role of starch in one pot fabrication of mesoporous gamma-alumina with excellent fluoride sorption capacity

Walter Ojok [a,b,c,*], Brenda Moodley [a], John Wasswa [d], Emmanuel Ntambi [b], William Wanasolo [e], James Bolender [f]

[a] School of Chemistry and Physics, University of KwaZulu-Natal, Westville Campus, Durban 4000, South Africa
[b] Department of Chemistry, Faculty of Science, Mbarara University of Science and Technology, P.O Box 1410, Mbarara, Uganda
[c] Department of Chemistry, Faculty of Science, Muni University, P.O Box 725, Arua, Uganda
[d] Department of Chemistry, College of Natural Sciences, Makerere University, P.O Box 7062, Kampala, Uganda
[e] Department of Chemistry, Faculty of Science, Kyambogo University, P.O Box 1 Kyambogo, Kampala, Uganda
[f] Department of Chemistry and Biochemistry, University of San Diego, 5998 Alcala Park, San Diego, CA 92110, USA

ARTICLE INFO

Keywords:
Green chemistry
Sol-gel
Response surface methodology
Nanoparticles
Kinetic
Thermodynamic study

ABSTRACT

Green synthesis of mesoporous γ-Al_2O_3, a cutting-edge material for sustainable application in medicine, engineering, energy, and water treatment, is still challenging. Our study used a one-pot strategy for facile synthesis of γ-Al_2O_3 by sol-gel method using starch from cassava waste. $Al(OH)_3$ were bound to the O-H groups of the starch molecule to form the $Al(OH)_3$-starch complex in a nano-network confined in starch polymer cages. Its calcination at 500 °C produced a mesoporous, highly crystalline water stable γ-Al_2O_3 with a pore size of 2.07 nm and an extensive BET surface area (215 cm^2/g). Using the response surface methodology (RSM), the as-synthesized γ-Al_2O_3 was optimized for efficient fluoride removal from water. A central composite design (CCD) was used to study the effect of initial fluoride concentration, pH, contact time, and sorbent dose on fluoride removal efficiency and optimization of the process. The relative importance of the sorption process variables to the fluoride removal process was assessed using ANOVA. The quadratic model showed that the predicted response was significantly correlated with the experimental response (R^2 = 0.9667), with sorbent dose and pH being the process's most influential factors. Optimum conditions for 93.6% fluoride removal efficiency were sorbent dose of 0.5 g, initial fluoride concentration of 10 mg/L, pH 7, and contact time of 137.5 min. A weakly acidic medium favored fluoride removal from water, while the presence of PO_4^{3-} and HCO_3^- retarded the process. The sorption data fitted well in the Langmuir isotherm (0.9783) and pseudo-second-order kinetic model (0.9999), indicative of a chemisorption process. The maximum sorption capacity towards fluoride was 207.5 mg/g. A thermodynamic study indicated that the sorption process was spontaneous and endothermic, with increased randomness at the solid-solution interface. Sorption, desorption, sustainability, and leaching tests showed that the sorbent could be used for sustainable fluoride removal at 8.3 USD/1000 liters of safe drinking water.

1. Introduction

Alumina and its composites continue to draw attention as cutting-edge materials in water treatment, production of biomedical devices, engineering ceramics, catalysis, lasers, lamps, and optical devices [1]. Their widespread use derives from their high strength, melting point, optical transparency, and abrasion resistance [2]. For example, in water treatment, aluminium oxide has a high affinity for fluoride ions and other contaminants due to its abundant active sites and can be a good sorbent for purification of contaminated water. Its high surface area-to-weight ratio enhances its sorption capacity towards such pollutants. Also, the Al^{3+} ion in alumina is a strong lewis acid and easily attracts electron-rich species, such as hydroxyl and fluoride ions [3]. Owing to these unique attributes, several attempts have been made to fabricate alumina and alumina composites for efficient fluoride sorption from water [2–4]. Although oxides of Ce, La, and Zr have been reported to have a remarkable affinity for fluoride ions due to their stability in various higher oxidation states and presence of enough vacant orbitals in them for accommodating fluoride ions [3,5], they are very expensive. This makes sorbent production using such metals precarious.

* Corresponding author at: School of Chemistry and Physics, University of KwaZulu-Natal, Westville Campus, Durban 4000, South Africa.
E-mail address: w.ojok@muni.ac.ug (W. Ojok).

https://doi.org/10.1016/j.scenv.2023.100034
Received 9 March 2023; Received in revised form 18 August 2023; Accepted 27 August 2023
Available online 28 August 2023

Abundance of aluminium in the earth's crust [6] makes it ideal for production of alumina for water treatment. Several studies revealed the potential of porous alumina with a high surface area for efficiently removing fluoride from water [2,3,6]. Despite these achievements, the conventional method of alumina production by precipitation using ammonia increases the problem of ammonium sulfate waste disposal and environmental pollution [7]. Efforts have been made to produce aluminium oxide with a high surface area and fluoride sorption capacity using polysaccharides to tackle this issue [8-10]. The numerous polar hydroxyl groups on polysaccharides make them ideal matrices for impregnation with Al^{3+} via electrostatic interactions, with capping and stabilizing attributes. Benefitting from these unique features, many researchers have fabricated alumina / composites for water treatment applications [2,3,8]. Alumina and its composites synthesized using polymeric matrices of chitosan, fumarate, cellulose and alginate have been widely used in removal of fluoride, arsenic, dyes and metal ions from contaminated water [2,9,11,12]. Despite these achievements, the preparation process is tedious and involves using expensive and toxic reagents, including surfactants. Starch, an alluring biopolymer has been shown to bind, host, protect, and tailor the structure of metal oxides during their synthesis. For example, Xu and co-workers [12] entrapped Zr^{4+} onto porous starch biopolymer to produce a sorbent with a remarkable fluoride sorption capacity of 25.41 mg/g. To improve on affordability, iron (instead of Zr) and cassava starch from cassava waste instead of commercial starch were used to synthesize hematite for fluoride removal [5]. These and other studies show the profound ability of metal oxide/oxyhydroxide nanoparticles from starch to remove fluoride and other pollutants from water. However, the lack of open mesopores and low pore volumes (< 0.73 nm) of some of the reported materials restricted the sorption capacity towards fluoride ions. Again, the low sorption capacity brought about by the slow diffusion rate of pollutants through the relatively small pore sizes is another concern [2,3,5]. To date, developing suitable sorbents with large pore sizes and ultrahigh sorption capacity towards fluoride and other water pollutants is still a challenge. To tackle this issue, a starch template has been used to fabricate mesoporous alumina as an advanced sorbent for water purification. The numerous hydroxyl groups in starch and their hydrophilic nature act as structure-directing agents for the supra-molecular interactions involving aluminium-starch composite. As a stabilizer, starch control particle size by preventing the spontaneous coalescing of aluminium oxide(oxyhydroxide) nanoparticles during their synthesis. Further, starch serves as a functionalizing agent by allowing the coordination of Al^{3+}ions to its numerous functional groups, making it a perfect templating agent for loading desired metal ions [8,13,14].

Developing a suitable sorbent for efficient water treatment provides solution for the challenge of water pollution [15,10,16] that the world is currently grappling with. Fluorine is a major water contaminant that occurs at elevated levels in groundwater in some countries in Central Asia, Sub-Saharan Africa, the United States of America, Southern Europe, and the Middle East [17,18]. Although fluorine is an essential trace element that is required in the human body for the formation of dental enamel and normal mineralization of skeletal structures [18], excess fluoride (>1.5 mg/L) may be hazardous to human health [19]. Ingestion of excess fluoride at a concentration > 1.5 mg/L can cause dental and skeletal fluorosis, growth retardation in children, lowering of IQ in children, neurological damage, infertility in women, and even death in extreme cases [20,21]. Hence remediation approaches ought to be taken to avert the health hazards of ingestion of excess fluoride, which is a global health risk. Sorption technique has proved to be a suitable means of purifying contaminated water due to its universal applicability, fast kinetics of binding, simple and inexpensive equipment, and ease of handling [3,6].

Herein, we report a facile one-pot synthetic approach for producing surfactant-free mesoporous alumina by the sol-gel method. This work involves the entrapment of Al^{3+} in a starch polymeric matrix followed by calcination of the resulting aluminium oxyhydroxide-starch composite at 500 ℃ to produce a mesoporous alumina. Starch is a widely used polysaccharide in the food industry with no known environmental/health-related hazards in materials synthesis [22]. Besides, the starch used in this study was obtained from cassava tuber waste, commonly generated while preparing fresh cassava for food. Additionally, benign reagents such as water, sodium hydroxide, and aluminium chloride were used in the protocol, which makes the protocol environmentally friendly and of low cost. To the best of our knowledge, the synthesis of mesoporous alumina using cassava starch as a soft template and its application in fluoride sorption have been reported for the first time. In this study, a central composite design (CCD) in response surface methodology (RSM) was used to examine the effects and interactions of four sorption process variables: initial fluoride concentration (A), contact time (B), pH (C), and sorbent dose (D) on fluoride removal efficacy by the as-synthesized γ-Al_2O_3. In addition, a multivariable quadratic regression model was developed to predict the fluoride sorption onto the γ-Al_2O_3 at different process conditions.

2. Experimental section

2.1. Materials

Aluminium chloride ($AlCl_3$), sodium hydroxide (NaOH), sodium fluoride (NaF), and hydrochloric acid (HCl) were purchased from Merck, Germany. Sodium chloride ($NaCl_)$, sodium nitrate ($NaNO_3$), sodium sulfate (Na_2SO_4), potassium hydrogen carbonate ($KHCO_3$), and sodium phosphate (Na_3PO_4) were purchased from Loba Chemie Pvt.Ltd., India. At the same time, the total ionic strength adjustment buffer (TISAB) was obtained from HACH company. All chemicals used were of high-purity analytical grade and used without further purification. Fresh cassava tubers were obtained from Cereleno Market in Gulu City, Northern Uganda. Experimental fluoride solution (stock and dilute) was prepared with ultrapure distilled water, and pH adjustments were made during the experiments with 0.1 M HCl or 0.1 M NaOH solutions. A standard stock fluoride solution containing 100 mg/L was prepared by dissolving 0.221 g of anhydrous sodium fluoride in ultra-pure distilled water to make 1 liter of solution. Standard fluoride solutions of various concentrations (10–100 mg/L) were prepared by diluting the stock solution with ultra-pure distilled water.

2.2. Synthesis of alumina

Alumina were synthesized by the sol-gel method. Briefly, dry cassava starch (20 g) was added to a 65 wt% aqueous aluminium chloride solution (100 mL) at 80℃ with constant stirring at 500 rpm on a magnetic hot plate. Then, a 15 wt% aqueous solution of sodium hydroxide was added dropwise to the mixture until pH 8 with constant stirring at 500 rpm. The mixture was then aged for 12 h while stirring at 80℃ to give an aluminium hydroxide-starch composite. The composite was filtered and washed meticulously with ultra-pure distilled water until pH 7 and dried in an oven at 110 ℃ for 12 h. Finally, the aluminium hydroxide-cassava starch composite was calcined at 500 ℃ for 3 h and gradually cooled to room temperature while in the furnace for 12 h to produce the as-synthesized alumina. The experiment was repeated using the same conditions but with 0, 5, 10, and 30 g of cassava starch.

2.3. Characterization of alumina

The surface texture and morphology of the Al_2O_3 were studied using a scanning electron microscope (FESEM, ZEISS EVO Series Scanning Electron Microscope Model EVO15, Jena, Germany) at an accelerating voltage of 5 kV and a transmission electron microscope (HRTEM, JEOL-1230). Elemental composition was analyzed using Energy Dispersive X-ray Spectroscopy (EDX). The phase composition and crystal structure were characterized by an X-ray powder diffractometer (XRD, D8 ADVANCE X) using Cu Kα (40 kV, 40 mA) radiation in the scanning

range of 10–80°. The Fourier-Transformed Infrared Spectrometer (Perkin Elmer, UK equipment) was used to study the chemical structure of the as-synthesized alumina in the wave number 400 – 4000 cm^{-1}. The specific surface area was calculated using the Brunauer-Emmett-Teller (BET) equation and Barret-Joyner-Hallender (BJH) from the nitrogen sorption-desorption isotherms determined by a Micro metrics Tristar II surface area and porosity analyzer. Zeta potential measurements were achived using a Malvern Zetasizer (ZS90, nanoseries Malvern Instruments Ltd, UK).

2.4. Sorption study

Jars containing 50 mL of fluoride solution with different initial fluoride concentrations (10 −100 mg/L), sorbent dosage (0.1–1.0 g), and pH (3 −12) were placed in an orbital shaker at 180 rpm at 25 ℃ at various contact times, for the kinetic study. For the equilibrium study, the sorption experiments were conducted using sorbent dose (0.5 g), initial fluoride (10 mg/L) and pH (7) and residual fluoride was determined after 12 h. The contents of the jars were then separated using Whatman number 1 filter paper (0.45 μm, Whatman, USA), and residual fluoride in each jar was determined using a Platinum series fluoride electrode (Model 51928–88, HACH Co., Ltd, Loveland, Colorado, U.S. A.). Finally, the efficacy of the as-synthesized γ-Al_2O_3 in removing fluoride from aqueous media was calculated using Eq. (1) [23]:

$$Fluoride \quad removal \quad (\%) = \frac{(C_0 - C_e)x100}{C_o} \tag{1}$$

$$Adsorption \quad capacity, Q = \frac{V \quad x(C_o - C_e \quad)}{1000x \quad m} \tag{2}$$

Where V (mL) is the volume of solution, m (g) is the mass of γ-Al_2O_3 used while C_0 and C_e were the initial fluoride concentration and equilibrium fluoride concentration in mg/L.

2.5. Desorption and reusability study

Desorption and reusability studies were performed by shaking the as-synthesized γ-Al_2O_3 (2 g) at 180 rpm with a fluoride solution (10 mg/L, 100 mL) for 12 h to attain equilibrium, and residual fluoride was determined as described earlier. After the sorption experiment in the first cycle, the spent sorbent was separated by centrifuging, and the residue was agitated with 1 M NaOH solution for 1 h. Lastly, the residue was dried at 110 ℃ and used in additional sorption experiments using the same procedure described in this section. The sorbent was regenerated four times in this experiment; each replicated three times.

2.6. Effect of co-existing anions and leaching tests experiments

The effect of co-existing anions SO_4^{2-}, NO_3^-, Cl^-, PO_4^{3-}, and HCO_3^- on fluoride removal using the as-synthesized γ-Al_2O_3 was studied by adding the co-existing anions (25 mL, 0.01 M) to fluoride solution (25 mL, 10 mg/L). The resulting solution was shaken with 0.5 g of the as-synthesized γ-Al_2O_3 for 12 h, and residual fluoride was determined as described earlier in this section.

2.7. Leaching tests experiments

The leaching experiment was carried out by shaking 2 g of the as-synthesized γ-Al_2O_3 with ultra-pure distilled water (100 mL) at 180 rpm for 12 h, followed by gravity filtration using Whatman number 1 filter paper (0.45 μm, Whatman, USA). The filtrate was then acidified with 1% ultra-pure nitric acid prior to determination of concentration of aluminium using a Perkin Elmer Optima 7300 DV Inductively Coupled Plasma- Optical Emission Spectrometer (ICP-OES). Ultra-pure distilled water was used as blank. The Perkin Elmer ICP-OES was precalibrated following the standard US EPA method 200.7 as described in the user's manual. The samples and blanks were analyzed with a Scotts spray chamber and a gem cone nebulizer. All the experiments were conducted in triplicate, and the mean values were reported.

2.8. Response surface methodology experimental design

In this study, experiments for fluoride removal using as-synthesized γ-Al_2O_3 were optimized using RSM. Response Surface Methodology enabled a systematic design of the experimental matrix in order to minimize wastage by using fewer experiments. In this study, the experimental design and the interactive effects of the process variables on the removal efficiency of fluoride ions by the as-synthesized γ-Al_2O_3 were modeled using the Central Composite Design (CCD) in Design Expert Software (Version 13.0.0, Stat-Ease Inc. Minneapolis, Minnesota, USA). The variables: initial fluoride concentration (A), contact time (B), pH (C), and sorbent dose (D) on fluoride removal efficiency by the as-synthesized γ-Al_2O_3 were selected as the independent sorption process parameters, and percentage fluoride removal as the response. Consequently, thirty experimental runs were designed based on the 2^n factorial points, 2 n axial points, and n center points (6 replications), that is.

$$\text{Number of experiments, } N = 2^n + 2n + 6 \tag{3}$$

3. Results and discussion

3.1. Synthesis of mesoporous alumina

Starch, a homoglycan containing amylose and amylopectin chains, provided numerous hydroxyl groups for bonding with the highly charged Al^{3+} ion. The addition of cassava starch to concentrated aluminium chloride solution produced a uniform viscous solution which suggested the interaction of Al^{3+} ions with the hydroxyl oxygen of the polysaccharide molecule to form an Al-starch complex, with subsequent hydrolysis of the glycosidic bonds [8] as represented in Fig. 1. The synthesis protocol for this study was optimized by varying the concentration of cassava starch while evaluating the resulting alumina's stability and fluoride removal performance. Twenty grams of cassava starch gave the most stable γ-Al_2O_3 with high fluoride removal efficiency.

As a result, more starch molecules dissolved as the intermolecular hydrogen bonds weakened to form a less viscous solution of the complex. Initially, hydroxy-functionalized layers of Al^{3+} could have interacted with polyol groups from starch via hydrogen bonding where the helical structure of starch encapsulated the Al^{3+} containing colloids [10]. When 15 wt% sodium hydroxide solution was added, the pH was raised and favored interaction of the species leading to the formation of $Al(OH)_3$-starch and $Al(OH)_3$ - $Al(OH)_3$ inclusion complexes after aging (Fig. 1). In the initial nucleation stage, the O-H functional groups on the starch bind to the $Al(OH)_3$, leading to the formation of the $Al(OH)_3$-starch complex in the nano-network. These nanonetworks controlled the growth, coagulation, and flocculation of the $Al(OH)_3$ particles as they could not move freely in the solution. In the absence of starch, the $Al(OH)_3$ particles could move freely, affecting the growth and coagulation of the particles to form a disordered array of clusters. The monodispersed controllable shape with well-defined morphology of the resulting alumina is attributed to the combined director effects of both the cassava starch and Al^{3+} ions [8]. Mesoporous alumina were obtained by calcinating the inclusion complexes at 500 ℃ in a muffle furnace. The average diameter of the prepared mesoporous alumina, as determined by the Scherrer equation (Eq. 3), ranged from 5.81 to 7.05 nm (Table 1). Since there were no diffraction peaks of cassava starch (at 15°) in the XRD spectra, it implies that starch wholly dissolved in the Al^{3+} ions [8].

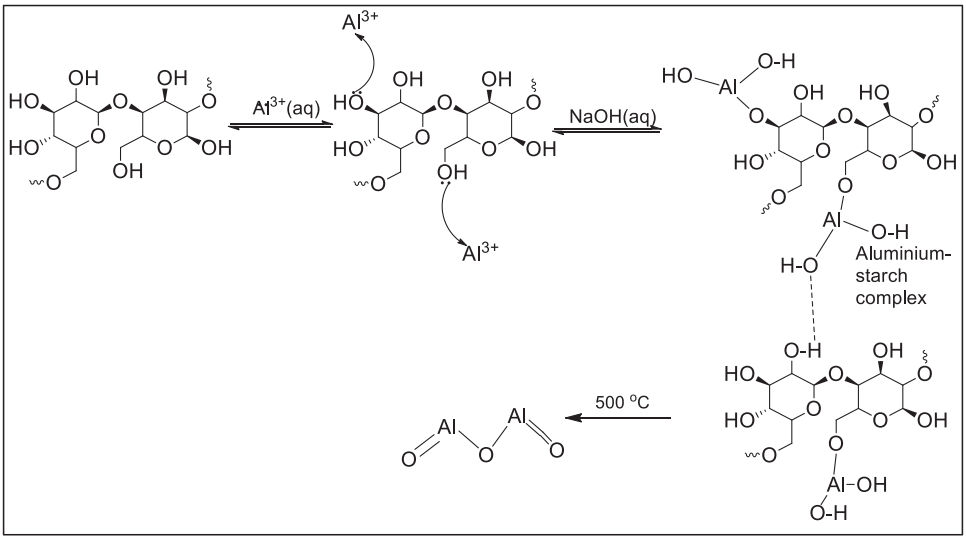

Fig. 1. Proposed mechanism for the formation of mesoporous γ-Al_2O_3.

Table 1
Lattice parameters of the as-synthesized γ-Al_2O_3.

Peak position (2θ)	θ (degrees)	Interplanar d spacing (Å)	Calculated a (Å)	Standard a (Å)	FWHM	Crystallite size, L (nm)	Miller indices h	K	*l*
31.6984	15.8492	2.8205	7.9776	7.9060	0.1892	7.0502	2	2	0
45.4181	22.7090	1.9953	7.9813	7.9060	0.1892	6.7606	4	0	0
56.4319	28.2160	1.6292	7.9816	7.9060	0.1892	6.4580	4	2	2
67.1369	33.5684	1.3931	7.8806	7.9060	0.1892	6.1066	4	4	0
75.1656	37.5828	1.2630	7.9878	7.9060	0.1892	5.8079	6	2	0

3.2. Characterization of alumina

3.2.1. X-ray diffraction

Wide angle X-ray diffraction (XRD) peaks of as-synthesized alumina were obtained at 2θ = 31.698°, 37.53°, 45.42°, and 67.14° corresponding to the reflection planes (220), (400), (422), (440) and (620) crystals of γ-Al_2O_3 (JCPDS card No: 01–077–0403). The presence of significant diffraction peaks only in the diffraction planes of γ-Al_2O_3 indicates the presence of pure face-centered cubic γ-Al_2O_3 structure in the sample. Again, the broadness of all the diffraction peaks indicates their fine nature with minimum degeneracy [24]. The crystallite size, L., of the synthesized alumina was calculated by the Debye-Scherrer Eq. (4) [23].

$$L = \frac{k\lambda}{\beta\cos\theta} \tag{4}$$

Where θ = Bragg's diffraction angle, L= diameter of the crystallite size, k = 0.90, λ (1.5406 nm) = wavelength of the x-rays of the Cu Kα radiation while β = full width at half maximum (FWHM).

The principal grain sizes of γ-Al_2O_3 prepared in the absence of cassava starch and with cassava starch calculated from the FWHM of the secluded diffraction peaks at (220), (400), (422), (440) and (622) reflection planes varied in the range of 5.81–7.05 nm (Table 1). The absence of any other significant diffraction peaks indicates that the γ-Al_2O_3 formed had a cubic structure and high purity.

The lattice parameter, a, was calculated using the following formula [4]:

$$a = d_{hkl}\sqrt{(h^2 + k^2 + l^2)} \tag{5}$$

where d_{hkl} is the interplanar spacing between two atomic planes, h, k, *l* are Miller indices related to unitary crystal cell, and *a* is the desired lattice parameter for face-centered cubic lattice structure. The calculated lattice parameter, *a*, for the γ-Al_2O_3 is close to the standard value for γ-Al_2O_3 from JCPDS 01–077–0403 (Table 1). The XRD patterns for alumina samples prepared in the absence of starch and one in the presence of starch are similar in peak positions but differ in intensities and broadness. This similarity indicates that samples synthesized in the presence of a cassava starch template exhibited high degeneracy and rough texture of the crystals [25].

3.2.2. Fourier transform infrared (FTIR) spectroscopy

Fig. 3 shows FTIR spectra of samples prepared in the absence of cassava starch and those prepared in the presence of cassava starch before and after fluoride sorption.

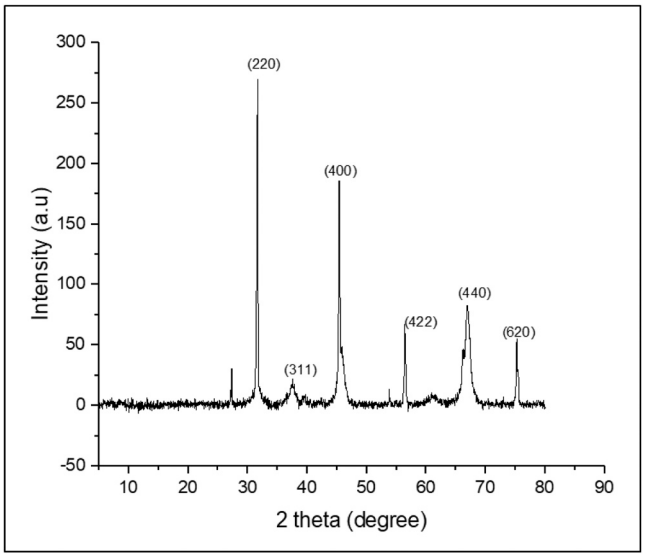

Fig. 2. XRD spectra of as-synthesized γ-Al_2O_3.

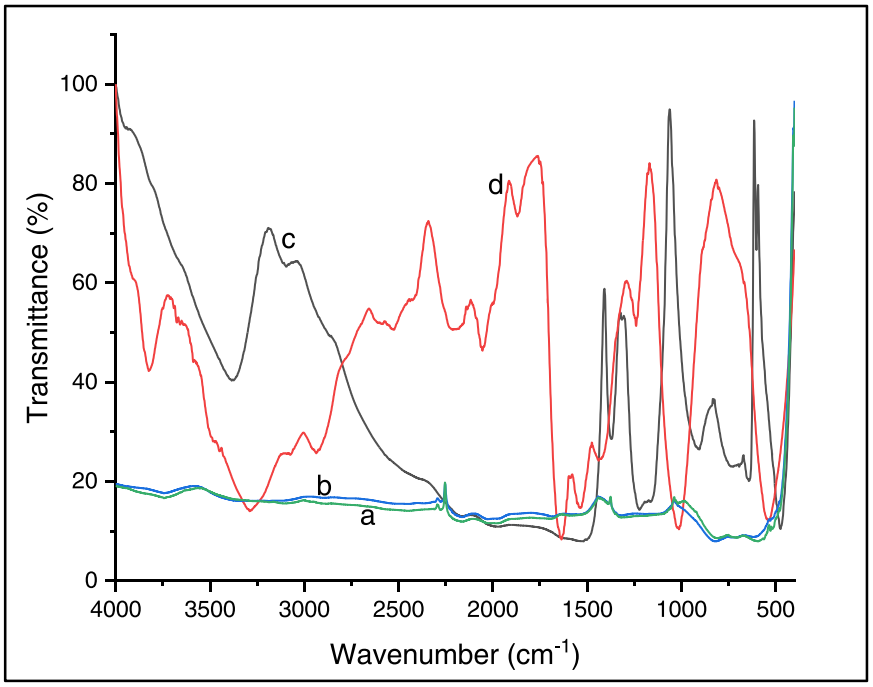

Fig. 3. FTIR spectra of (a) Al_2O_3 prepared without cassava starch, (b) as-synthesized γ-Al_2O_3 prepared using cassava starch before fluoride sorption, (c)) as-synthesized γ-Al_2O_3 after fluoride sorption (d) pristine cassava starch.

Fig. 3 shows broad peaks in the wavenumber range of 3200–3400 cm^{-1} due to the stretching vibrations of the O-H group. This peak is very intense in Fig. 3(d) due to numerous OH groups from starch. The significant but less intense peak in Fig. 3(c) was due to the sorption of water molecules. The asymmetric stretch of the acetal groups at 1645 cm^{-1} was strong in pristine starch (Fig. 3d) but diminished in Fig. 3(b & c).

Similarly, the intense peak at 1025 cm^{-1} (Fig. 3(c) is attributed to vibration bands of the C-O-C bonds of the α-1,4-glycosidic linkages between the glucose units in cassava starch. All these bands have

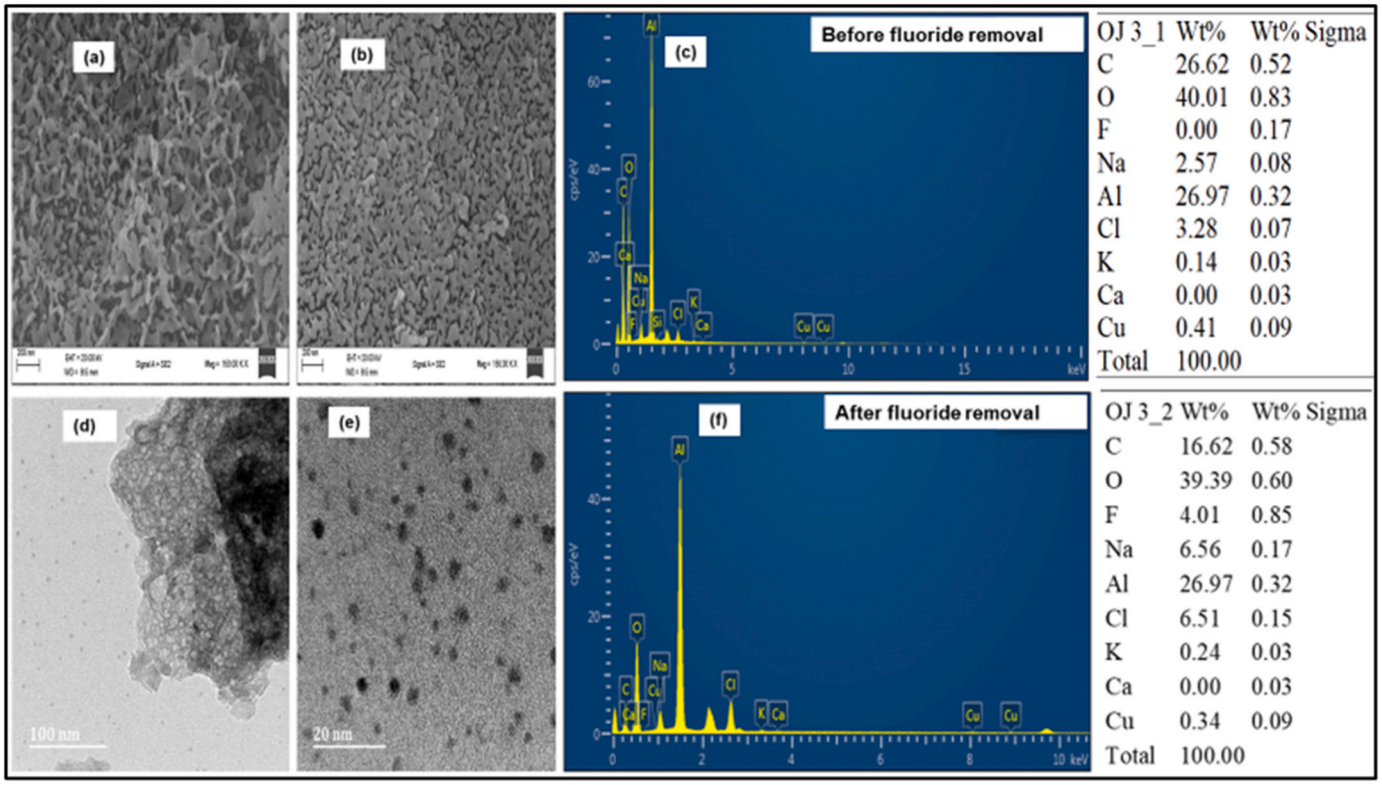

Fig. 4. (a) SEM image of alumina prepared using cassava starch (γ-Al_2O_3)before and (b) after fluoride sorption, (c) EDX spectrum of alumina before fluoride sorption, (d-e)TEM image of alumina (f) EDX spectrum of alumina after fluoride.

diminished or disappeared in the final calcined gamma-alumina sample (Fig. 3(b). Furthermore, broad peaks were observed at 840 and 740 cm^{-1} in Fig. 3(a, b & c) due to the stretching vibrations of the Al-O-Al, Al-O-H, and Al-O bonds [25]. The appearance of very broadband in this region is due to the ordered distribution of vacancies for the γ-Al_2O_3 as a result of incomplete crystallization of γ-Al_2O_3. This is a result of the coordination of the acetal group in starch to the Al^{3+} ions, as represented below [26].

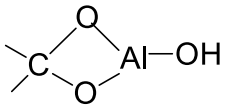

.

The FTIR data obtained in this study further buoyed the formation of γ-Al_2O_3. Additional peaks at 1230 cm^{-1} and 630 cm^{-1} after fluoride sorption (Fig. 3(c) was due to the formation of Al – F and Al-O-H-F bonds [3].

3.2.3. Microscopic characterization of synthesized alumina

SEM image (Fig. 4(a)) of the as-synthesized γ-Al_2O_3 shows rough surface morphology with a uniform size distribution of particles and a worm-like structure with an approximate size below 100 nm. The rough surface of the as-synthesized γ-Al_2O_3 possibly accounts for the sorption of fluoride ions. Such rough surfaces with increased textural porosity bear more active sites and facilitate the diffusion of sorbates, thus leading to enhanced sorption and chemical reactions. The porosity reduced after fluoride sorption as indicated in Fig. 4(b), due to the occupancy of sorption sites on alumina by fluoride ions and the $\pi -$ electrostatic interactions [6]. The presence of F in the energy dispersive x-ray spectroscopy (EDX) spectrum in the γ-Al_2O_3 sample after fluoride sorption further proves that the synthesized alumina seized fluoride ions from the aqueous media (Fig. 4(c,f). The rough morphology of the as-synthesized γ-Al_2O_3 agrees with previous works [27] and is suited for fluoride sorption.

TEM image of the as-synthesized alumina prepared using cassava starch as a soft template shows a porous worm-like appearance (Fig. 4(d-e). From the TEM micrographs obtained, the particle size for the as-synthesized γ-Al_2O_3 was less than 100 nm. This finding is in line with the crystallite sizes obtained in XRD analysis.

3.2.4. Brunauer-Emmett-Teller (BET) and Barret-Joyner-Hallender (BJH) analysis

Nitrogen sorption-desorption analysis was conducted to study the surface area and pore size distribution on the as-synthesized γ-Al_2O_3. The as-synthesized γ-Al_2O_3 shows a typical type IV sorption isotherm (Fig. 5(a) which indicates its mesoporous nature. Pore size distribution curves obtained from the adsorption branch were analyzed by the BJH method, indicating a pore size of 0.30–2.07 nm, ideal for efficient fluoride sorption. The BET-specific area and total pore volume of the as-synthesized γ-Al_2O_3 were 215 m^2/g and 0.20 cm^3/g, respectively, uniquely suited for fluoride sorption [2].

The mesopores in the alumina provided paths for the diffusion of fluoride ions which possess a small ionic radius of 0.147 nm. Whereas a lower surface area of 139 $m^2.\ g^{-1}$ was achieved for γ-Al_2O_3 prepared from sodium aluminate liquor with polyethylene glycol, a comparable surface area of 201 $m^2.\ g^{-1}$ of alumina was obtained using polyvinyl alcohol as a surfactant [25]. Furthermore, mesoporous alumina of higher surface areas (260–464 m^2/g) than alumina in the current study was prepared using different saccharide molecule templates [28]. A much lower surface area of 5.4 $m^2.\ g^{-1}$ was obtained for alpha alumina nanoparticles prepared by sol-gel method in a study by Niero et al. [29]. This finding further underpins the vital role of hydroxyl groups (O-H) on the cassava starch biopolymer in structure directing and facilitating anisotropic growth of the alumina to give well-defined mesoporous γ-Al_2O_3 with high specific surface area. The high surface area of the as-synthesized alumina provided numerous active sites for fluoride sorption.

3.3. Zeta potential and sorption of fluoride ion onto the as-synthesized γ-Al_2O_3 at different pH

The zeta potential of the as-synthesized γ-Al_2O_3 decreased with an increase in pH value, showing that the electrical charges at the sorbent surface depended on the pH value of the media (Fig. 6(a). The pH of the solution also influences the chemical form of fluoride and the surface chemistry of the sorbent [30,31]. Therefore, the zeta potential of the as-synthesized γ-Al_2O_3 and the effect of pH on fluoride removal was studied over the pH range of 3–12. From Fig. 6(a), fluoride sorption varied significantly with a variation in solution pH. At low pH < 5, fluoride removal was low because there could be the preferential formation of AlF_x. Fluoride removal increased with an increase in pH as this phenomenon decreased when the predominant chemical form of

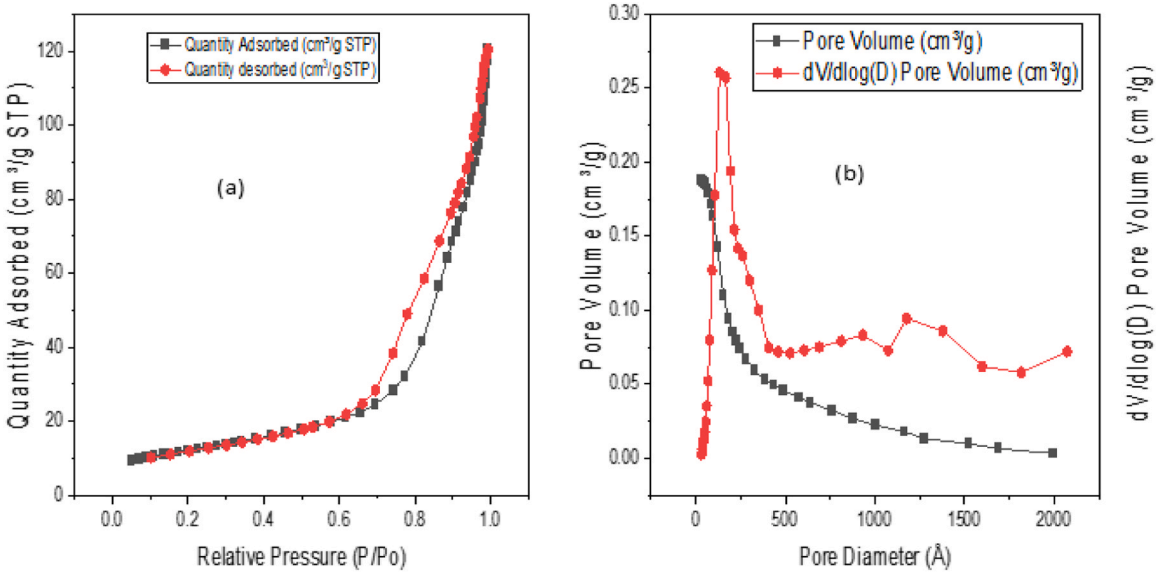

Fig. 5. (a) BET N_2 adsorption-desorption isotherm for the as-synthesized γ-Al_2O_3 (b) Pore size distribution for the as-synthesized γ-Al_2O_3.

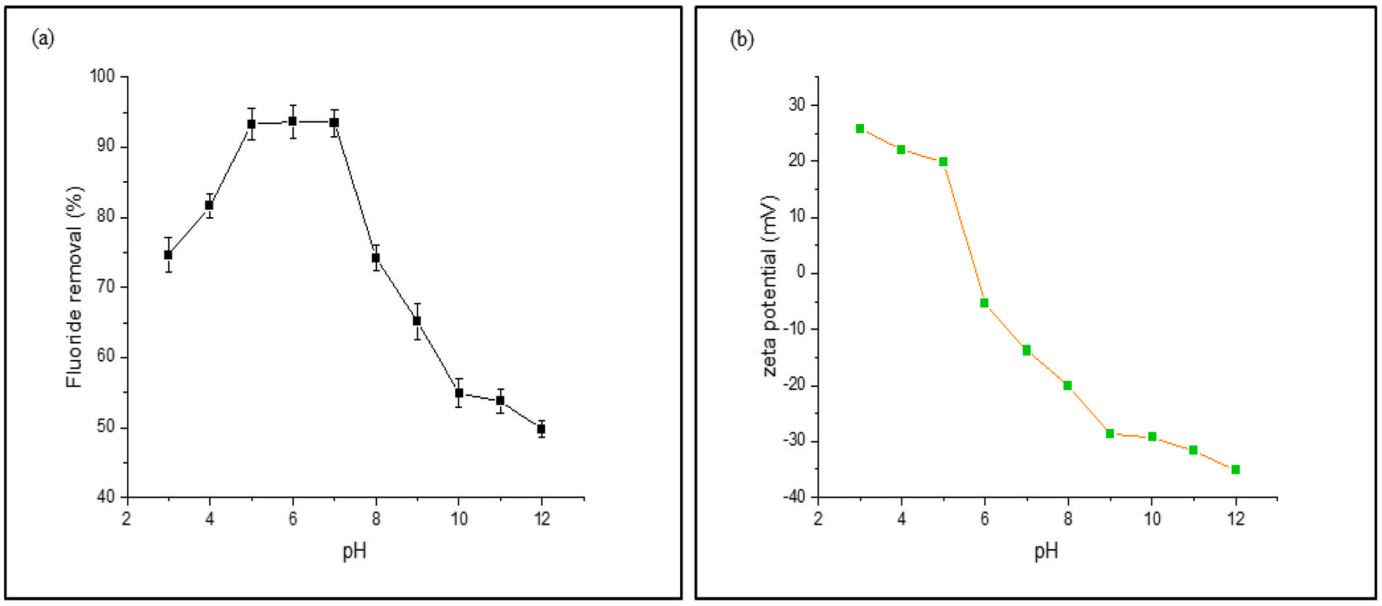

Fig. 6. (a) Effect of pH on fluoride sorption onto as-synthesized γ-Al_2O_3 (b) Variation of zeta potential of as-synthesized γ-Al_2O_3 with pH.

fluorine changed from HF to F^- ions. Also, in weakly acidic media, there is protonation of the surface of the sorbent, which makes the sorption of anionic species like fluoride possible. The maximum percent fluoride removal (93.6%) occurred in pH 5–7 (Fig. 6b). After reaching the maximum value of 93.6% at pH 7, the sorption capacity decreased rapidly. This decrease may be attributed to the competition of hydroxyl

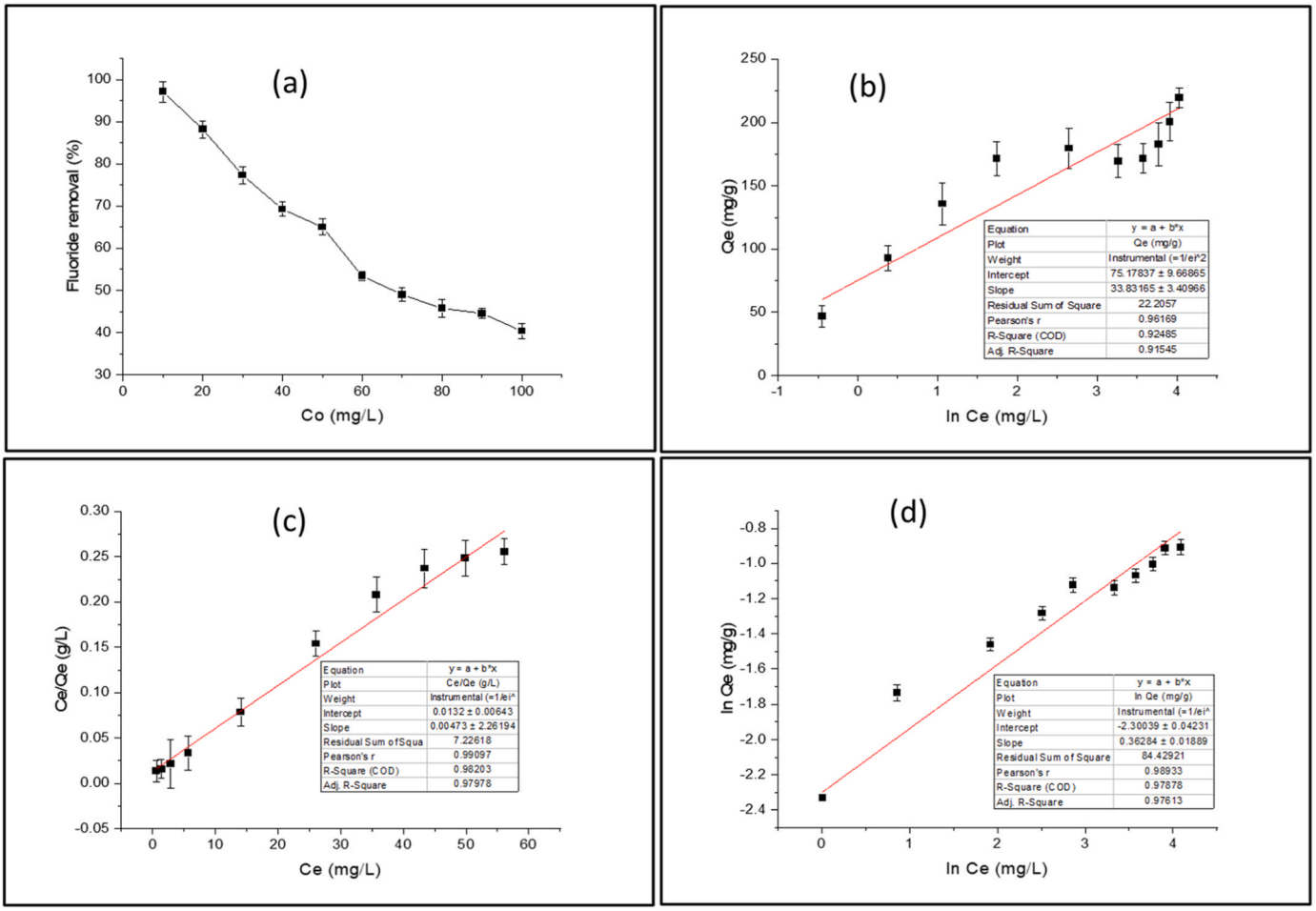

Fig. 7. Equilibrium isotherms for fluoride sorption onto as synthesized γ-Al_2O_3 (a) Effect of initial fluoride concentration (b) Temkin isotherm model (c) Langmuir isotherm model and (d) Freundlich isotherm model.

ions in the solution with F^- ions at pH > 7.

3.4. Sorption equilibrium and isotherms study

The effect of initial fluoride concentration on the fluoride removal capacity of as-synthesized γ-Al_2O_3 was carried out in the range of 10–100 mg/L, with a sorbent dose of 0.5 mg/L, pH 7, and room temperature. The percent of fluoride removed for the various initial fluoride concentrations is presented in Fig. 7(a). The percentage of fluoride removed decreased with an increase in initial fluoride concentration. This phenomenon may be ascribed to insufficient availability of the as-synthesized γ-Al_2O_3 active sites at higher initial fluoride concentrations. Conversely, at lower initial fluoride concentrations, the active sites on the as-synthesized γ-Al_2O_3 were abundant and accessible to fluoride ions. Previous studies obtained similar results [31].

The sorption equilibrium data were fitted into the Temkin & Pyzhev [32], Langmuir [32], and Freundlich [33] isotherm models, the most commonly used models to examine the phenomenon of fluoride sorption. Table 2 and Fig. 7(b, c, d) display the results for the parameters obtained from the three isotherm models.

The Temkin isotherm is given by Eq. (6):

$$Q_e = B\ln K_T + \ln C_e \tag{6}$$

where: C_e= equilibrium concentration of sorbate, K_T = Temkin isotherm equilibrium binding constant (L/g), R= Universal gas constant (8.314 J/mol /K), T = Temperature at 298 K, B= Temkin isotherm constant.

This isotherm uses the heat of sorption to classify the adsorption process as physisorption or chemisorption. It assumes that the heat of sorption of all molecules in a layer decreases linearly rather than logarithmically for an intermediate sorbate concentration with coverage on the sorbent surface [32]. A careful look at the Temkin plot (Fig. 7(d) reveals three stages of the sorption process. Initially, the heat fall for the first four points was linear, while the next stage, comprising two points, involves a decrease in heat fall and other points representing an exponential increase in heat fall. These results may indicate that an initial formation of a monolayer coverage occurs when the initial concentration of fluoride is low (≥ 50 mg/L), with a probable multilayer formation at high initial fluoride concentrations [32]. Furthermore, the calculated values of Temkin isotherm parameters K_T (16.028 L/g) and B (29.8833 J/mol) indicate that the enthalpy change associated with the binding of fluoride to the as-synthesized γ-Al_2O_3 is favorable for the sorption of fluoride on the sorbent.

The linearized form of the Langmuir isotherm is given in Eq. (7):

$$\frac{1}{\mathrm{Qe}} = \frac{1}{K_b Q_m}\left(\frac{1}{\mathrm{Ce}}\right) + \frac{1}{Q_m} \tag{7}$$

where: Q_e= sorbed amount of fluoride concentration (mg /g), Q_m= maximum sorption capacity of the as-synthesized γ-Al_2O_3 for fluoride ions, C_e= equilibrium concentration of aqueous fluoride (mg/L), K_L = measure of the affinity of fluoride ions for the as-synthesized γ-Al_2O_3.

This isotherm assumed that monolayer sorption on a homogenous surface of the as-synthesized γ-Al_2O_3 continues to occur until maximum sorption capacity reaches saturation with all available sorption sites occupied by the fluoride ions but without adjacent interactions between sorbed fluoride ions. The sorption data of this study fitted best to the Langmuir model (Fig. 7(c) and Table 2), with correlation coefficient R^2 = 0.97827 and a maximum sorption capacity (Q_m) of 207.5 mg/g, much higher than that of other alumina based sorbents reported for fluoride sorption [6,34]. Furthermore, an additional Langmuir constant, R_L, called the separation factor, which indicates whether the sorption of fluoride onto the as-synthesized γ-Al_2O_3 is favorable or not, is given by the expression in Eq. (8).

$$R_L = \frac{1}{(1 + K_L C_o)} \tag{8}$$

Generally, a good sorption process is indicated by $0 < R_L < 1$, linear sorption is indicated by R_L= 1, while R_L> 1 and R_L= 0 show unfavorable sorption and irreversible sorption, respectively [35]. This study obtained a separation factor, R_L, of 0.036, which indicated favorable fluoride sorption onto the as-synthesized γ-Al_2O_3.

Freundlich isotherm described multilayer sorption of fluoride ions over the as- γ-Al_2O_3 with a heterogeneous surface[33]. A linear form of the Freundlich isotherm is given in Eq. (9).

$$Q_e = \ln K_f + \frac{1}{n}\ln C_e \tag{9}$$

where Q_e = amount of fluoride sorbed per unit weight of γ-Al_2O_3 (mg/g), C_e= equilibrium concentration of aqueous fluoride (mg/L), K_f= Freundlich constant (L/g) indicative of the relative sorption capacity of the as-synthesized γ-Al_2O_3, n = a measure of how an affinity for the sorbate changes with a change in adsorption density. Fitting the sorption data of this study to Eq. (8) gave a regression coefficient, R^2 = 0.9429.

For a value of n = 1, the Freundlich isotherm becomes a linear isotherm, showing that all the sorption sites on the sorbent have equal affinity for the fluoride ions. However, values of n> 1 indicate that affinities of sorbent for the sorbate ions decrease with increasing sorption density [33]. In this study, the value of n = 3.17 obtained indicated favorable sorption of fluoride ions onto the as-synthesized γ-Al_2O_3 with a heterogeneous surface. However, sorption efficiency decreased as sorption sites accumulated fluoride ions while the value of 1/n = 0.315 was obtained, indicating a chemisorption process [33]. The best fitting of the sorption data into the Langmuir model is consistent with other reports for fluoride sorption using alumina-based sorbents [2]. Although some of the sorbents reported in the literature achieved similar sorption capacities or even higher values, the narrow pH range and use of aggressive chemicals in their synthesis limit their utilization in fluoride removal. For example, an aluminium-fumarate metal-organic framework with a sorption capacity of 596 mg/g was reported in a study by Kumari et al. [11]. However, using polyvinyl alcohol as a surfactant and fumaric acid as a binder renders the protocol environmentally unsafe. This problem is excellently dealt with in the current study. Our method used cassava starch instead of synthetic binders in a sol-gel method to produce an efficient fluoride sorbent (γ-Al_2O_3) with high porosity and surface area for fluoride sorption. Table 3.

Table 2
Sorption Isotherm Parameters of Fluoride using γ-Al_2O_3 (N = 3, Relative standard deviation, RSD < 5%).

Isotherm	Parameter	Value
Temkin	B (J/mol)	29.8833
	R^2	0.8422
	K_T(L/g)	16.028
Langmuir	Q_m (mg/g)	207.46
	K_L (L/mg)	2.6660
	R_L	0.0360
	R^2	0.9783
Freundlich	K_f (mg/g) (L/mg)$^{1/n}$	55.8891
	N	3.17
	R^2	0.9429
	1/n	0.3154

3.5. Sorption kinetic study

The sorption kinetics analysis was used to appraise the efficiency of fluoride sorption onto the as-synthesized γ-Al_2O_3. At different contact times, sorption experiments were done at three initial fluoride concentrations (10, 50, and 100 mg/L). As depicted in Fig. S2(a), the percent of fluoride removed increased rapidly at first due to abundant unoccupied sorption sites at the beginning of the sorption process. Finally, the

Table 3
Comparison of performance of different alumina-based sorbents used for fluoride removal from water.

Sorbent	Template used	Optimum pH	Maximum sorption capacity (mg/g)	Reference
Al_2O_3 @chitosanHPMC	Chitosan,Hydroxymethylcellulose(PMC)	-	125.1	[36]
Cactus-like amorphous Al_2O_3 microsphere	Solvothermal without template	5–8	129.4	[37]
Al_2O_3 @CaO	Triblock copolymer pluronic P123	5	450	[38]
Al_2O_3 @chitosan	Chitosan	5–9	8.3	[39]
Al(OH)3 @cellulose	Cellulose nanofibril	5–10	35	[40]
Al-fumarate MOF	Polyvinyl alcohol, chitosan and fumaric acid	3–7	596	[11]
Al@ABDC-chitosan	2-aminobenzene-1,4-dicarboxylic acid(ABDC),deacetylated chitosan	7	5.0	[41]
γ-Al_2O_3	Cassava starch	5–7	207.5	This study

equilibrium was attained at around 137 min with the different initial fluoride concentrations at a temperature of 25 ℃. As shown in Table 4, $Q_{e,exp}$ increased from 0.936 mg/g to 4.035 mg/g as initial fluoride concentration increased from 10 mg/L to 100 mg/L. In order to estimate the rate of fluoride sorption and the phenomenon of mass transfer onto the as-synthesized γ-Al_2O_3, the experimental kinetic data were fitted into the Lagergren pseudo-first-order, the Lagergren pseudo-second-order kinetic, Weber-Morris intra-particle diffusion and the Elovich kinetic equations.

The Lagergren pseudo-first-order [42] equation is given in Eq. S1 (Supplementary information). The plot in Fig. S2(b) and $R^2 = 0.48594$ showed that the data did not fit well into the pseudo-first-order model. The pseudo-second-order model, which assumes that the rate-limiting step in the sorption process involves chemisorption, is given in Eq. (S2) [42].

A plot of $\frac{t}{Q_t}$ against t was made, and the results are shown in Fig. S2(c) and Table 4. The correlation coefficients for pseudo-second-order are closer to 1 ($R^2 = 0.9999$) than that of pseudo-first order, Elovich, and the Weber- Morris intraparticle diffusion models. Moreover, the experimental sorption capacity, $Q_{e,exp,}$ is in good agreement with the theoretical value, $Q_{e,\ cal,}$ for this model, suggesting that the fluoride sorption onto the as-synthesized γ-Al_2O_3 involved chemisorption. Eq. (S3) represents the Elovich kinetic model. A graph of Q_t against t was plotted (Fig. S2(d) and values of β and α were calculated with results presented in Table 4.

Although the linear regression coefficient (R^2) values of the Elovich model were lower than for second-order kinetics, they are higher than those for the pseudo-first-order kinetic model and the Weber-Morris model, meaning that the sorption data for this study fit better in the Elovich model than the latter, indicating a chemisorption process [9, 40].

The Weber-Morris intra-particle diffusion model is given in Eq. (S4) [43], and associated model parameters are given in Table 4. As seen in Fig. S2(e) and Table 4, intra-particle diffusion had negligible influence on the sorption kinetics due to the mesoporous nature and small particle size of the as-synthesized γ-Al_2O_3.

3.6. Mechanism of fluoride removal by as-synthesized γ-Al_2O_3

The process of fluoride sorption onto as-synthesized γ-Al_2O_3 involves electrostatic attraction, hydrogen bonding, ion exchange, and complexation [3], broadly categorized as physisorption and chemisorption processes. This is because the surface of alumina is amphoteric due to the presence of coordinately unsaturated Al^{3+} ions and "acidic" hydroxy groups contributing to acidity and basic sorption sites arising from the presence of O^{2-} ions and basic hydroxy groups [44].

In the present study, the involvement of chemisorption is indicated by the results of pseudo-second-order kinetics and the Langmuir isotherm fit. The chemisorption mechanism involved electronic interactions by distribution or exchange of electrons between the fluoride ions and the as-synthesized γ-Al_2O_3. This may occur via the complexation of fluoride ions with dissolved aluminium oxide/hydroxo species to form fluoroaluminates and hydrogen bonding. For example, when the as-synthesized γ-Al_2O_3 is added to an aqueous fluoride solution, the lone pairs of electrons on the oxygen of the sorbent attract protons from water molecules to form hydroxyl ligands on the sorbent surface. At low pH, the hydroxyl ligands on the as-synthesized γ-Al_2O_3 become protonated and thus positively charged. Electrostatic forces attract the negatively charged fluoride ions to the positively charged $AlOH_2^+$ species [6].

$$AlOH_2^+ + F^- \rightleftharpoons AlOH_2^+ \ldots F^-$$

Also, due to similarity in size and charge, F^- ions replaced the OH^- ions in the sorbent structure; the F^- ions became attached to the sites initially holding the OH groups as the OH^- ions were released into the solution [4] as is evident from the FTIR spectra in Fig. 2(b).

.

Sorption by hydrogen bonding involves the polar hydroxyl functional groups on the as-synthesized γ-Al_2O_3. The unequal displacement of electrons leaves the hydrogen atom in the O-H bond partially positive,

Table 4
Kinetics Parameters for the Sorption of Fluoride onto the as-synthesized γ-Al_2O_3.

Kinetic model	Initial fluoride concentration (mg/L)	Kinetic constant	$Q_{e,exp}$ ($mg.g^{-1}$)	$Q_{e,cal}$ ($mg.g^{-1}$)	R^2
Pseudo-first order	10	0.0002377 min^{-1}	0.936	1.329	0.48594
	50	0.5201 min^{-1}	3.25	3.7	0.39003
	100	0.54623 min^{-1}	4.035	40	0.19253
Pseudo-second order	10	0.5325 $g.mg^{-1}.min$	0.936	0.9441	0.99997
	50	0.1743 $g.mg^{-1}.min$	3.25	3.702	0.99998
	100	1.25 $g.mg^{-1}.min$	4.035	6.558	0.99999
Intra-particle diffusion	10	$K_{id} = 0.006616$			0.42248
	50	$K_{id} = 0.02001$			0.40907
	100	K_{id}= 0.00547			0.24957
	Initial Fluoride conc.(mg/L)	B	α		R^2
Elovich	10	2.6685	7.37805		0.77178
	50	16.3300	4.51800		0.76365
	100	36.9600	28.2400		0.53700

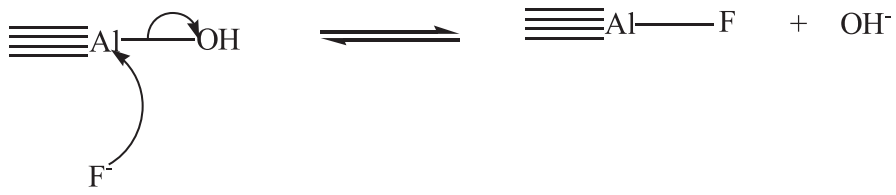

thereby attracting the electron-rich F^- ions from the solution [11].

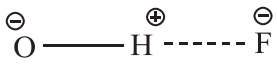

.

At higher pH 5–7, there was immobilization of F^- ions on the as-synthesized γ-Al_2O_3 through a series of complexation reactions involving fluoroaluminate species (AlF^{2+}, AlF_2^+), hydroxo-aluminium species (AlOH) on the surface of the synthesized alumina, and hydrogen bonding [3].

$$AlOH + AlF^{2+} \rightleftharpoons AlOH - AlF^{2+}$$

$$AlOH + AlF_2^+ \rightleftharpoons AlO\,H - AlF_2^+$$

$$AlOH_2^+ + F^- \rightleftharpoons AlOH_2^+ - F^-$$

$$AlOH + F^- \rightleftharpoons AlOH - F^-$$

3.7. Thermodynamics study

The effect of temperature on the sorption of fluoride onto as-synthesized γ-Al_2O_3 was studied at 303, 313, and 323 K, and initial fluoride concentrations of 10, 50, and 100 mg/L. The maximum percentage of fluoride removed by the as-synthesized γ-Al_2O_3 occurred at 303 K. Thermodynamic parameters: enthalpy change (ΔH), entropy change (ΔS), and Gibbs free energy change (ΔG) were determined using Eqs. (10)–(12):

$$K = \frac{C_{ad}}{C_e} \tag{10}$$

$$\ln K = -\frac{\Delta H}{R}\left[\frac{1}{T}\right] + \frac{\Delta S}{R} \tag{11}$$

$$\Delta G = -RT\ln K \tag{12}$$

where K, ΔH (J/mol), R (8.314 J/mol K), T(K), ΔS (J/mol/K), ΔG (J/mol), C_e (mg/L), and C_{ad} (mg/L) are the equilibrium constant, enthalpy change, molar gas constant, absolute temperature, entropy change, Gibbs free energy change, the concentration of fluoride ions in solution at equilibrium and amount of fluoride sorbed onto as-synthesized γ-Al_2O_3 at equilibrium, respectively.

The values of the thermodynamic parameters presented in Table 5 were calculated from the slope and intercept for each initial fluoride concentration (Fig. S2). These parameters provide information on the nature of the sorption process observed in this study.

Table 5
Thermodynamic Parameters for Sorption of Fluoride onto as-synthesized γ-Al_2O_3.

Initial fluoride concentration (mg/L)	ΔH (J/mol)	ΔS (J/mol/K)	ΔG (J/mol)		
			303 K	313 K	323 K
10	7.36	46.53	-6852.07	-7182.30	-7760.87
50	11.90	42.70	-1060.56	-1441.66	-1917.39
100	16.92	37.34	-486.19	-197.77	-604.22

The value of ΔG decreased with an increase in temperature (Table 5) for all the initial fluoride concentrations. The negative ΔG values for all the temperatures and initial fluoride concentrations mean that fluoride sorption onto the as-synthesized γ-Al_2O_3 was feasible and imprudent. This means that at high temperatures, the value of ΔG decreased with consequent improvement in fluoride sorption. This phenomenon is because higher temperature lowers the solution's volume expansion and viscosity, increasing mass transfer from the liquid phase to the solid interface. Generally, values of $0 \leq \Delta G \leq -20,000$ J/mol indicate physisorption process whereas $-80{,}000 \leq \Delta G \leq -400{,}000$ J/mol show chemisorption. In the present study, the values of ΔG were in the range of 0 J/mol to $-20,000$ J/mol, indicating that the fluoride removal process by the as-synthesized γ-Al_2O_3 involved physisorption [5,31].

At the same time, the positive values of ΔH obtained in this study were below 40 kJ/mol, signaling that the sorption process is physisorption and endothermic [45]. The value ΔS decreased with an increase in initial fluoride concentration. The positive value of ΔS indicate that the randomness increase at the solid-liquid interface. The increase in randomness is due to the displacement of sorbed water molecules by the fluoride ions to attain more translational entropy than is lost by the fluoride ions, thereby allowing for a high degree of randomness in the system.

3.8. Response surface methodology study

3.8.1. Optimization of fluoride sorption onto as -synthesized γ-Al_2O_3

The 3D surface plots of the effect of two independent process variables on fluoride sorption when all the other process variables were kept constant are presented in Fig. 8 while intensity of interations are given by the contour plots in Fig. 9. The incline of the 3D surface plots indicates the strength of the interaction of the two independent variables under consideration [46]. The interactive effect of contact time and initial fluoride concentration (Fig. 8(a) shows an inclined curve indicating a significant interplay between the two factors. However, contact time had a more significant effect on fluoride removal efficiency than initial fluoride concentration, with an increase in contact time improving fluoride sorption. This is because an increase in residence time allows fluoride ions to diffuse to the active sites on the sorbent. In contrast, an increase in initial fluoride concentration had an insignificant effect on the fluoride sorption process. In fact, with a high initial fluoride concentration, fluoride sorption capacity reduces due to the saturation of the active sites with fluoride ions on the sorbent surface, and no further sorption takes place. Therefore, an increase in contact time from 52.5 to 137.5 min and an initial fluoride concentration from 32.5 to 77.5 mg/L results in a sustained fluoride removal percentage of up to 74%.

Similarly, an interactive plot for pH and initial fluoride concentration (Fig. 8b) is a little flat, showing that the interplay between the factors is insignificant. According to Fig. 8(b), pH had a more significant effect on fluoride removal than initial fluoride concentration. A low pH (5.25–7.05) favors fluoride sorption, but cooperatively, a sorption efficiency of about 73% was attained. The interactive plot for as-synthesized γ-Al_2O_3 dose and pH (Fig. 8(c) indicates significant synergistic effects of the two variables on fluoride removal efficiency, with as-synthesized γ-Al_2O_3 dose having greater influence. This effect is because

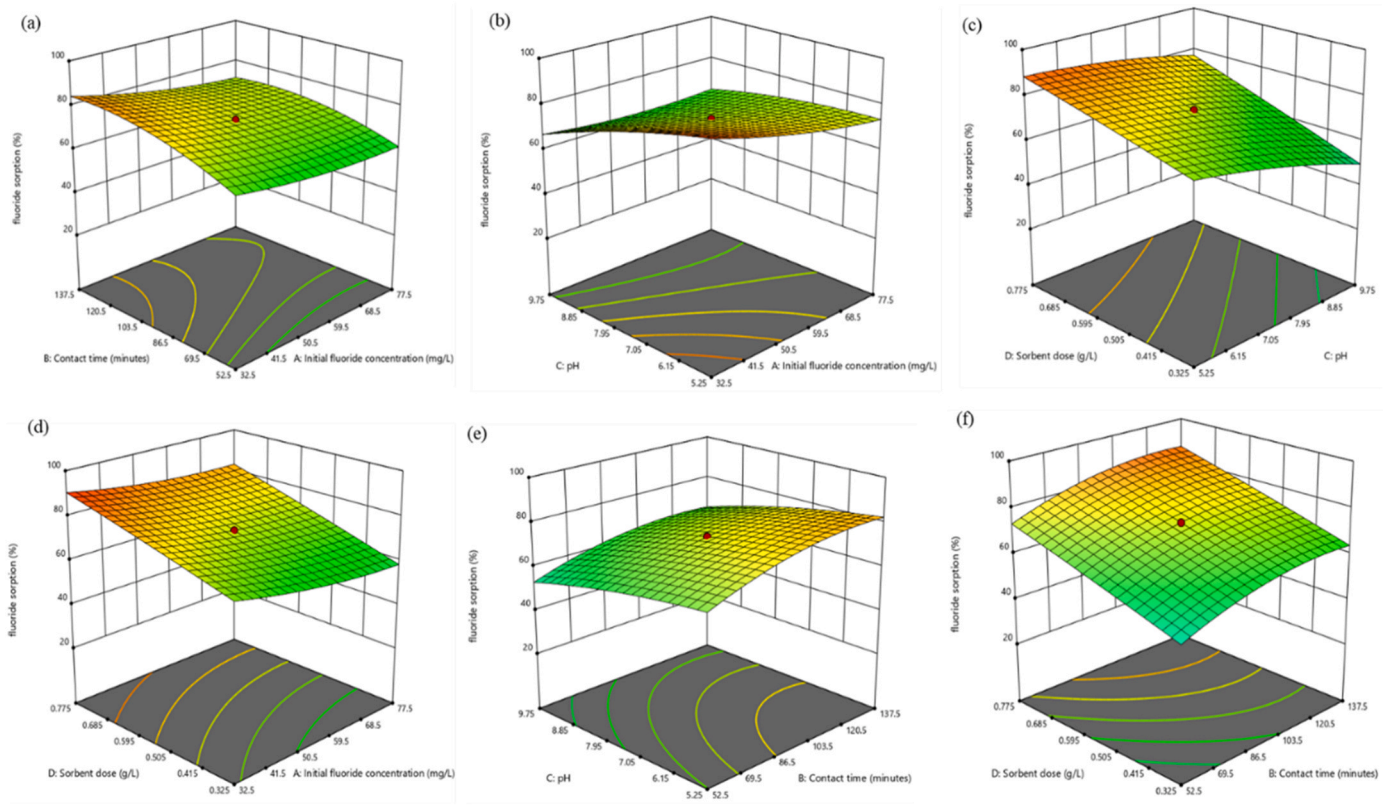

Fig. 8. 3D surface plot showing the effect of (a) contact time and initial fluoride concentration (b) pH and initial fluoride concentration (c) as-synthesized γ-Al_2O_3 dose and pH (d) as-synthesized γ-Al_2O_3 dose and initial fluoride concentration (e) pH and contact time (f) as-synthesized γ-Al_2O_3 dose and contact time, on fluoride sorption process.

an increase in sorbent dose provides more active sites for fluoride uptake from the solution [47]. When the as-synthesized γ-Al_2O_3 dose was increased from 0.325 g to 0.775 g and pH from 5.25 to 9.25, the fluoride removal efficiency was 74%. Interactive plot for as-synthesized γ-Al_2O_3 dose and initial fluoride concentration in (Fig. 8(d) and contour plot in Fig. 9(d) show a cooperative effect on fluoride removal efficiency, with sorbent dose having a more significant influence on the process. Notably, a high amount of γ-Al_2O_3 dose significantly increased fluoride sorption efficiency while increasing initial fluoride concentration had a lesser effect. The increase in sorbent dose from 0.325 g to 0.775 g and initial fluoride concentration from 32.5 mg/L to 77.5 mg/L led to a fluoride removal efficiency of 89%.

Fig. 8(e) displays a significant interaction between pH and contact time, with an increase in contact time having the most significant effect on fluoride removal efficiency. Their combined effect resulted in the lowest fluoride removal efficiency of approximately 65%. The most excellent cooperative effect was exhibited in the interactive plot for the as-synthesized γ-Al_2O_3 dose and contact time (Fig. 8f), with an increase in both factors improving fluoride removal tremendously. An increase in γ-Al_2O_3 dose from 0.325 to 0.775 g and contact time from 52.5 to 137.5 min resulted in a fluoride removal efficiency of 93.6%. From the optimization study, maximum fluoride removal can be achieved with an initial fluoride concentration of 10 mg/L, contact time of 137.5 min, pH of 7.0, and as-synthesized γ-Al_2O_3 dose of 0.5 g/L. The results discussed here indicate that each factor affects fluoride removal efficiency differently.

3.8.2. *Model development for sorption of fluoride onto the as-synthesized γ-Al_2O_3*

The central composite design (CCD) was optimized for fluoride sorption onto the as-synthesized γ-Al_2O_3. An experimental design matrix composed of thirty experiments was developed using the CCD approach. In addition, a multivariable data-driven model was developed to predict fluoride removal efficiency for different amounts of the process variables. The quadratic model shows the numerical relationships between independent variables and percentage fluoride removal in Eq. (13).

$$\textit{Fluoride sorption (\%)} = +88{\cdot}19845 - 1{\cdot}25927\,A + 0{\cdot}618098\,B - 7{\cdot}43457\,C + 50{\cdot}50\,D + 0{\cdot}071235\,A{*}C + 0{\cdot}004721\,A^2 - 0{\cdot}002421\,B^2 \quad (13)$$

The independent process variables *A, B, C,* and *D* are initial fluoride concentration, contact time, pH, and amount of the as-synthesized γ-Al_2O_3. Positive signs of the coefficients in the model show synergistic effects, while the negative sign of coefficients denotes opposing or antagonizing effects. Analysis of variance (ANOVA) for the fluoride removal efficiency by the as-synthesized γ-Al_2O_3 (Table 6) suggests that initial fluoride concentration, contact time, pH, and sorbent dose were all significant model terms. These terms were checked with p-values and F-values. Therefore, *A, B, C, D, A*C, A^2,* and B^2 are significant model terms.

In addition, the predicted coefficient of determination R^2(0.6676) is in reasonable agreement with adjusted R^2(0.8250) with a difference of < 2 with a p-value ($<$0.0001) and F-value of 20.53 indicating that the model terms are significant. The adequacy of precision measures signal-to-noise ratio, and a value > 4 is desirable. Therefore, the adequacy of 17.30 obtained in this study shows that the model developed can be used to navigate the design space since there is a sufficient signal in the model with negligible noise (errors). A plot of predicted values Vs. actual values (Fig. 8) also approve that the developed model is an earnest predictor of fluoride sorption onto the as-synthesized γ-Al_2O_3. As seen in Fig. 8, most predicted values were near to the experimental data. Hence, the model (Eq. 13) could be practically and dependably applied for predicting fluoride removal percentage using the as-synthesized γ-Al_2O_3 at the stated independent variable levels.

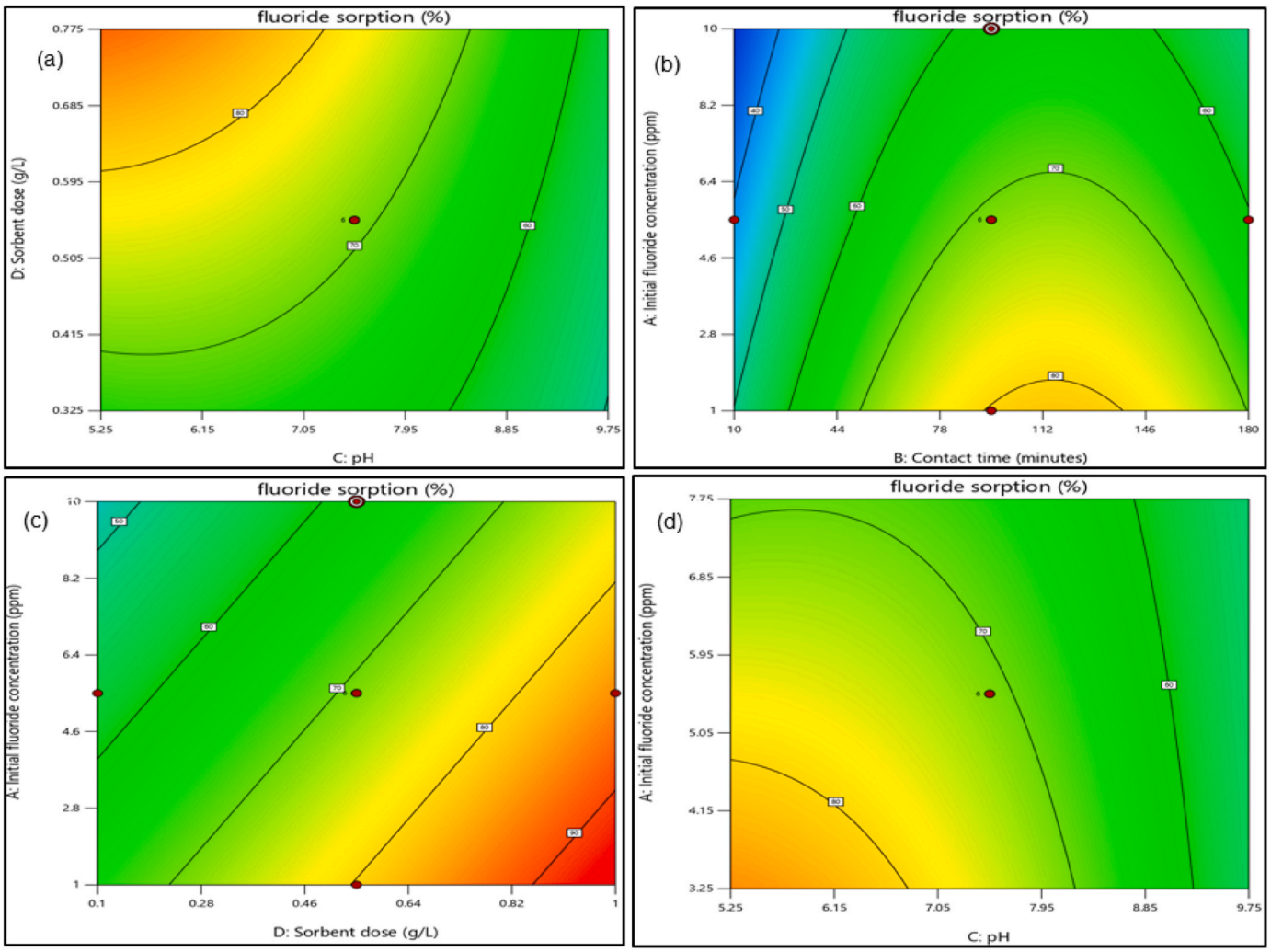

Fig. 9. Contour plots showing the (a) effect of sorbent dose and pH (b)initial fluoride concentration and contact time (c) initial fluoride concentration and sorbent dose (d) initial fluoride concentration and pH on the efficiency of the γ-Al_2O_3 for fluoride removal.

Table 6
Analysis of variance for the quadratic model for fluoride sorption onto the as-synthesized γ-Al_2O_3.

Source	Sum of Squares	df	Mean Square	F-value	p-value	
Model	7189.62	7	1027.09	20.53	< 0.0001	significant
A-Initial fluoride concentration	514.30	1	514.30	10.28	0.0041	
B-Contact time	1084.07	1	1084.07	21.67	0.0001	
C-pH	1502.58	1	1502.58	30.04	< 0.0001	
D-Sorbent dose	3098.55	1	3098.55	61.95	< 0.0001	
AC	208.08	1	208.08	4.16	0.0536	
A^2	162.46	1	162.46	3.25	0.0852	
B^2	543.86	1	543.86	10.87	0.0033	
Residual	1100.37	22	50.02			
Lack of Fit	1100.37	17	64.73			
Pure Error	0.0000	5	0.0000			
Cor Total	8289.99	29				

According to the F-value, the degree of influence of the variables was in the order sorbent dose > pH > contact time > initial fluoride concentration.

3.8.3. Validation of the model for fluoride sorption process onto as-synthesized γ-Al_2O_3

Three fluoride sorption experiments were conducted at the optimized values of the process variables for maximum fluoride removal of 93.6% by the as-synthesized γ-Al_2O_3 of initial fluoride concentration = 10 mg/L, pH = 7, and γ-Al_2O_3 dose = 0.5 g at a contact time of 137.5 min. The experiments were repeated three times to verify the prediction, and the results are given in Table 7. The experimental values for fluoride removal using γ-Al_2O_3 agree with the model-predicted values with a standard deviation (S.D)≤0.025.

3.8.4. Effect of co-existing anions

A study on the effects of common anions in groundwater: SO_4^{2-}, NO_3^-, Cl^-, PO_4^{3-}, and HCO_3^- on fluoride removal using the as-synthesized γ-Al_2O_3 showed that PO_4^{3-} and HCO_3^- affected fluoride removal efficiency drastically while the SO_4^{2-}, NO_3^- and Cl^- had a slight effect on fluoride sorption.

Table 7
Model validation at optimum conditions.

	Optimum parameters				Fluoride removal %		
Experiment	Initial F⁻conc. (mg/L)	pH	dose: (g)	Contact time (min.)	Experimental	Predicted	SD
1	10.01	7.02	0.50	137.5	83.65	83.71	0.025
2	10.00	7.00	0.52	137.6	83.60	83.58	0.01
3	10.02	7.03	0.51	137.4	83.39	83.41	0.01

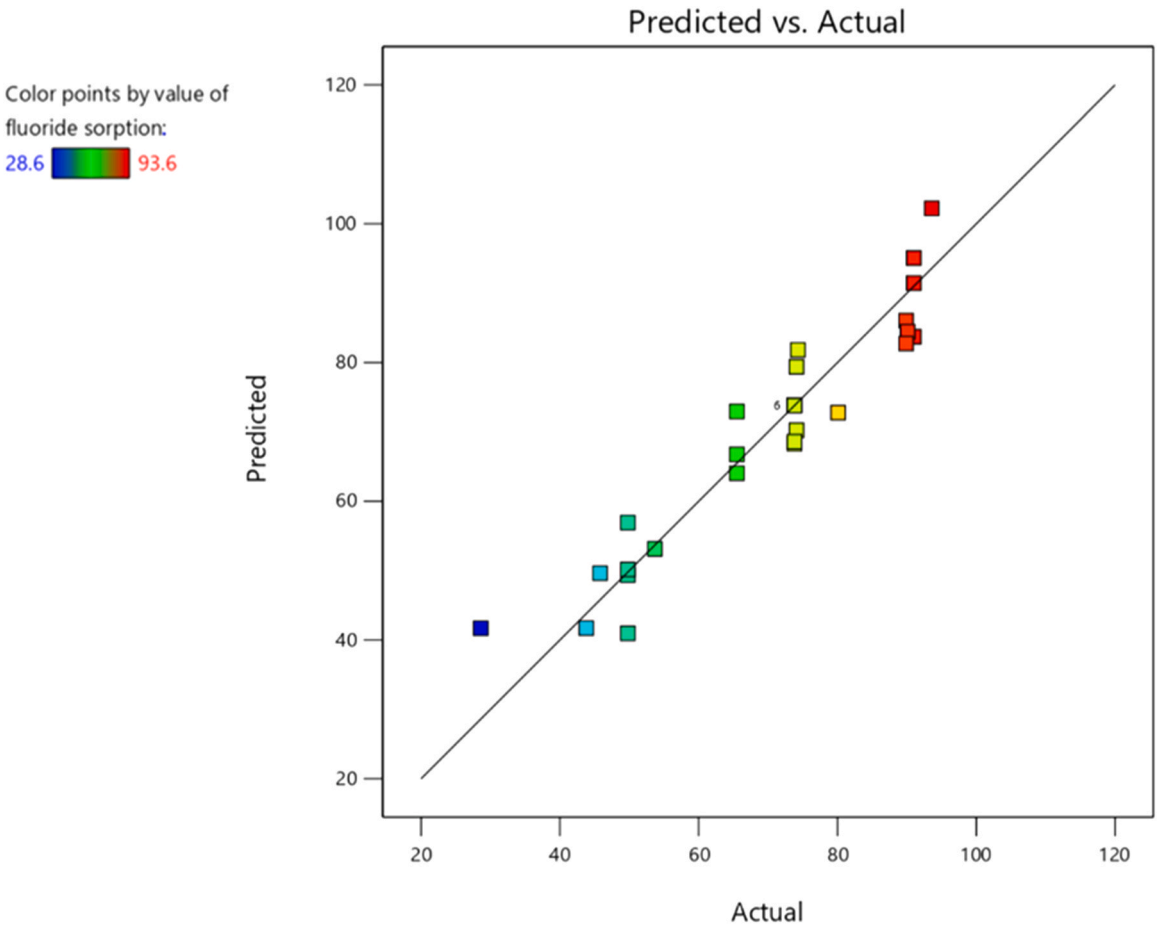

Fig. 10. Comparison of model-derived and experimental fluoride sorption.

Fig. 11(a) displays the effect of co-existing anions considered in this study. The adverse effects of the anions: PO_4^{3-} and HCO_3^- on fluoride sorption is due to anion hydrolysis involving these anions leading to the release of hydroxide ions, which raises the pH of the solution and similarity in anionic size of the HCO_3^- ions [30]. The increased pH creates negative charges on the sorbent, causing electrostatic repulsion of incoming fluoride ions, thereby reducing fluoride sorption efficiency.

3.8.5. *Desorption and sustainability study*

Regeneration of sorbent for its reusability is essential in determining its economic advantage. The as-synthesized γ-Al_2O_3 was successfully desorbed by shaking the spent sorbent with 0.1 M sodium hydroxide solution. The sorbent was recycled four times, and the sorption/desorption cycles are depicted in Fig. 10(b). The as-synthesized γ-Al_2O_3 retained 67.5% of its fluoride removal ability in the fourth cycle, indicating that the as-synthesized alumina had remarkable reusability and can be considered for practical application in defluoridation. Furthermore, the spent γ-Al_2O_3 can be safely dumped at the city landfill since the γ-Al_2O_3 is stable in water meaning its aluminium will be released gradually and has low acute toxicity.

3.9. *Sustainable chemistry metrics*

The sustainability of synthesis and application of the as-synthesized γ-Al_2O_3 in fluoride removal was studied by evaluating the green chemistry metrics viz energy intensity, environmental factor, mass intensity, water intensity, and affordability. The sustainable chemistry metrics for the as-synthesized γ-Al_2O_3 were calculated using standard equations [45,48], and the results are given in Table 8.

3.9.1. *Greenness of raw materials and synthesis protocol used*

Cassava starch is a renewable plant material, and aluminum chloride has low acute toxicity, while sodium hydroxide is corrosive but not flammable. The acidic Al^{3+} from the salt neutralized the sodium hydroxide during the reaction forming the γ-Al_2O_3, sodium chloride, and water, which are less harmful products. Water was the only solvent used

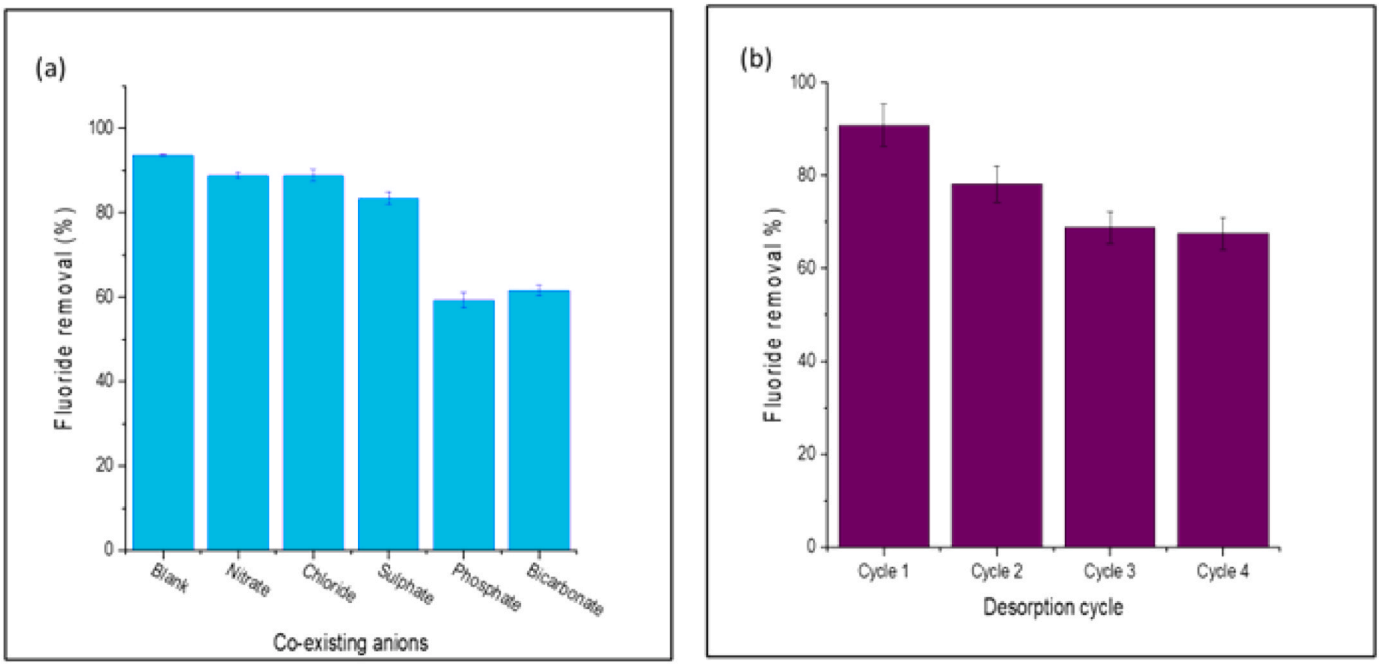

Fig. 11. (a) Effect of co-existing anions on fluoride removal using γ-Al_2O_3 (b) Desorption efficiency of the as-synthesized γ-Al_2O_3.

Table 8
Sustainable Chemistry Metrics for the synthesis of the γ-Al_2O_3.

Parameter	Quantity
E-factor(kg of waste/kg of product)	0.3
Energy intensity(kW.h/kg of product)	4.5
Mass intensity (kg/kg of product)	7.4
Water intensity (kg/kg of product)	40

and could be easily recycled. Hence all the raw materials are benign and easily acquired, and the synthesis procedure was generally green.

3.9.2. *Environmental factor (E-factor)*

Effective use of raw materials was assessed using the E-factor, calculated using the Eq. (S8). An ideal value of zero shows full conformity with green chemistry, while higher E-factor values indicate the generation of high volumes of waste and vice versa [46]. A value of 0.3 obtained in our study shows that a low quantity of waste is generated in the protocol.

3.9.3. *Energy intensity*

The energy intensity was calculated using Eq. (S5). An approximate value of 4.5 kW.h of electricity was used to produce 1 kg of γ-Al_2O_3, mainly for oven drying, centrifuging, and calcination. Mass production of the γ-Al_2O_3 and sun drying of the cassava starch and γ-Al_2O_3 could reduce energy costs.

3.9.4. *Mass and water intensity*

The mass and water intensity values were calculated using Eqs. (S7) and (S6), respectively. A mass intensity of 7.4 kg/kg obtained in this study was higher than that obtained in a study by Egor et al.[47]. Reducing the loss of synthesized γ-Al_2O_3 during washing and filtration could improve the mass intensity value. An approximately 40 kg/kg value for water intensity obtained in this study is similar to the findings of related works [47]. Recycling water used for washing is one way to reduce this relatively high-water intensity value.

3.9.5. *Cost of technology*

Fluoride sorption using the as-synthesized γ-Al_2O_3 showed that fluoride levels in water could be reduced to below 1.5 mg/L at approximately 8.3 USD/1000 liters of safe drinking water in batch experiments. This cost is slightly higher than that reported for a similar study [47] but cheaper than the membrane technology.

3.9.6. *Leaching tests for Al and stability of the as-synthesized γ-Al_2O_3*

The stability of the synthesized sorbent in water is an important parameter affecting its utilization in defluoridation. The amount of aluminium leached into the treated water was evaluated using a Perkin Elmer Optima 7300 DV Inductively Coupled Plasma- Optical Emission Spectrometer (ICP-OES). Deionized water before and after contact with the γ-Al_2O_3 was acidified with 5% nitric acid prior to measurement of Al in a precalibrated Perkin Elmer ICP-OES following the standard US EPA method 200.7. The amount of Al leached into the water was in the range of 0.1–0.22 mg/L. The sample prepared using 20 g of cassava starch gave the best balance between fluoride removal efficiency and stability and was used to produce sorbent for the sorption experiments. The protocol used to synthesize the γ-Al_2O_3 for the sorption experiments was one with Al leaching 0.12 mg/L, which is below the WHO (2017) limit of 0.2 mg/L for drinking water. The leaching tests further indicate that the aluminium hydroxide was incorporated in the starch polymer matrix and, thus, not easily leached into the water. Table 9

4. Conclusions

Mesoporous γ-Al_2O_3 was successfully synthesized by sol-gel method

Table 9
Effect of cassava starch concentration on the stability and aluminium leaching of the synthesized sorbent.

Sample	Amount of cassava starch added	Stability	Al leached (mg/L)	Fluoride removal (%)
1	0 g	Very poor	0.22	96.6
2	5 g	Poor	0.2	95.1
3	10 g	Good	0.15	94.0
4	20 g	Good	0.12	93.6
5	30 g	Very good	0.1	89.7

using starch from cassava waste and applied to sustainably remove fluoride ions from water. The suggested mechanism for forming the alumina-starch involved the interaction of the Al^{3+} with polyhydroxy groups of starch to form an aluminium-starch inclusion complex which transformed to mesoporous Al_2O_3 after aging and calcination. The mechanism of fluoride removal was proposed to be anion exchange, hydrogen bonding, surface complexation, and electrostatic interaction. Response surface methodology was used to optimize the fluoride sorption onto γ-Al_2O_3 with an initial fluoride concentration of 10 mg/L, pH = 7, γ-Al_2O_3 dose = 0.5 g at a contact time of 137.5 min found to give maximum fluoride removal of 93.6%. ANOVA test indicates that the developed quadratic model is statistically significant. Fluoride removal efficiency increased with an increase in sorbent dose, contact time, and pH (3−7) but decreased with an increase in initial fluoride concentration above 32.5 mg/L.

The fluoride sorption was well modeled by the pseudo-second-order kinetic model and the Langmuir isotherm model with a maximum sorption capacity of 207.46 mg/g, indicating efficient monolayer sorption on a homogeneous surface. The presence of PO_4^{3-} and HCO_3^- decreased the fluoride removal efficiency of the as-synthesized γ-Al_2O_3. Also, the thermodynamic study indicates the sorption process was spontaneous, endothermic, and entropy-driving. The as-synthesized sorbent showed excellent desorption properties and reusability in four cycles. Green chemistry metrics of the γ-Al_2O_3 evaluated and showed its protocol's greenness and the treated water cost is expected to be affordable. Therefore, the as-synthesized γ-Al_2O_3 can be a potential sorbent for the sustainable defluoridation of fluoride-ladened water.

Declaration of Competing Interest

The authors declare that they have no known competing financial interests or personal relationships that could have appeared to influence the work reported in this paper.

Data availability

Data will be made available on request.

Acknowledgment

The authors gratefully acknowledge the African-German Network of Excellence in Science (AGNES) and the German Academic Exchange Service (DAAD) [Grant number: 91672385] for funding the study. In addition, the authors are grateful for the instrumentation and technical support from the School of Chemistry and Physics, University of KwaZulu-Natal, Westville Campus, Durban in South Africa, particularly the Microscopy Unit. W.O also thank Mr. Ajay Bissesur for his assistance with the crucibles for calcinating the composite. Finally, W.O is grateful to all members of the Analytical /Physical Chemistry and the Nano Research Groups for their enormous help in accessing the various laboratories and with instrumentation and company during the fellowship period. W.O was a Ph.D. student at the Department of Chemistry, Mbarara University of Science and Technology, Mbarara (Uganda), and was an AGNES research fellow in 2021 at the School of Chemistry and Physics, University of KwaZulu-Natal, Westville Campus.

Appendix A. Supporting information

Supplementary data associated with this article can be found in the online version at doi:10.1016/j.scenv.2023.100034.

References

[1] K. Davis, Material review: alumina (Al 2 O 3), Sch. Dr. Stud. Eur. Union J. no. 2 (2010).
[2] S.I. Alhassan, L. Huang, Y. He, L. Yan, B. Wu, H. Wang, Fluoride removal from water using alumina and aluminum-based composites: A comprehensive review of progress, Crit. Rev. Environ. Sci. Technol. (2020) 1–35.
[3] Y. Wei, L. Wang, H. Li, W. Yan, J. Feng, Synergistic fluoride adsorption by composite adsorbents synthesized from different types of materials—a review, Front. Chem. vol. 10 (May) (2022) 1–23, https://doi.org/10.3389/fchem.2022.900660.
[4] C. Yu, et al., Fluoride removal performance of highly porous activated alumina, J. Sol. -Gel Sci. Technol. (2022) 1–9.
[5] W. Ojok, E. Ntambi, J. Bolender, J. Wasswa, W. Wanasolo, B. Moodley, Synthesis and characterization of hematite biocomposite using cassava starch template for aqueous phase removal of fluoride, Carbohydr. Polym. Technol. Appl. vol. 4 (2022), 100241, https://doi.org/10.1016/j.carpta.2022.100241.
[6] C. Yu, et al., Fluoride removal performance of highly porous activated alumina, J. Sol. -Gel Sci. Technol. vol. 106 (2) (2023) 471–479, https://doi.org/10.1007/s10971-022-05722-2.
[7] Y. Wu, P. Xu, L. Li, Synthesis of alumina with coarse particle by precipitating aluminum ammonium sulfate solution with ammonia, Adv. Powder Technol. vol. 27 (1) (2016) 124–129.
[8] N. Shah, W.A. Khan, T. Rehan, D. Lin, H. Tetik, S. Haider, 12 - polysaccharides-metal oxide composite: a green functional material, in: S. Haider, A.B.T.-R. P., P.-M.O.C. Haider (Eds.), Metal Oxides, Elsevier, 2022, pp. 371–394.
[9] S.K. Swain, et al., Removal of fluoride from aqueous solution using aluminum-impregnated chitosan biopolymer, Sep. Sci. Technol. vol. 44 (9) (2009) 2096–2116.
[10] X. Li, H.Y. Yang, A global challenge: clean drinking water, Glob. Chall. vol. 5 (1) (2021).
[11] R. Kumari, A. Kumar, S. Basu, Aluminium fumarate-based polymer matrix composite for selective removal of fluoride from groundwater, Environ. Nanotechnol., Monit. Manag. vol. 17 (2022), 100642, https://doi.org/10.1016/j.enmm.2022.100642.
[12] L. Xu, G. Chen, C. Peng, H. Qiao, F. Ke, R. Hou, Adsorptive removal of fluoride from drinking water using porous starch loaded with common metal ions Adsorptive removal of fluoride from drinking water using porous starch loaded with common metal ions, Carbohydr. Polym. vol. 160 (March) (2017) 82–89, https://doi.org/10.1016/j.carbpol.2016.12.052.
[13] A.D. Gupta, K.P. Rawat, V. Bhadauria, H. Singh, Recent trends in the application of modified starch in the adsorption of heavy metals from water: a review, Carbohydr. Polym. vol. 269 (2021), 117763.
[14] W. Ojok, J. Wasswa, C.K. Nakiguli, and E. Ntambi, Spatial variation in physicochemical surface water quality in River Rwizi, Western Uganda, 2019.
[15] W. Ojok, J. Wasswa, E. Ntambi, Assessment of seasonal variation in water quality in River Rwizi using multivariate statistical techniques, Mbarara Municipality, Uganda J. Water Resour. Prot. vol. 9 (1) (2017) 83–97.
[16] W. Ojok, W. Wanasolo, J. Wasswa, J. Bolender, E. Ntambi, Hydrochemistry and fluoride contamination in Ndali-Kasenda crater lakes, Albertine Graben: Assessment based on multivariate statistical approach and human health risk, Groundw. Sustain. Dev. (2021), 100650.
[17] P.K. Jha, P. Tripathi, Arsenic and fluoride contamination in groundwater: a review of global scenarios with special reference to India, Groundw. Sustain. Dev. (2021), 100576.
[18] WHO. Guidelines for Drinking-water Quality, Fourth edi.,, World Health Organization,, Geneva, 2017.
[19] P.L. Smedley et al., Fluoride in groundwater from high-fluoride areas of Ghana and Tanzania, 2002.
[20] P. Bhattacharya, et al., Health risk assessment of co-occurrence of toxic fluoride and arsenic in groundwater of Dharmanagar region, North Tripura (India), Groundw. Sustain. Dev. vol. 11 (2020), 100430.
[21] L. Yuan, et al., Health risk in children to fluoride exposure in a typical endemic fluorosis area on Loess Plateau, north China, in the last decade, Chemosphere vol. 243 (2020), 125451.
[22] M.I.U. Hoque, et al., A Facile Synthesis of Hematite Nanorods from Rice Starch and Their Application to Pb(II) Ions Removal, ChemistrySelect vol. 4 (13) (2019) 3730–3736, https://doi.org/10.1002/slct.201802462.
[23] K. Biswas, S.K. Saha, U.C. Ghosh, Adsorption of fluoride from aqueous solution by a synthetic iron (III)− aluminum (III) mixed oxide, Ind. Eng. Chem. Res. vol. 46 (16) (2007) 5346–5356.
[24] Z. Zhang, T.J. Pinnavaia, Mesoporous γ-alumina formed through the surfactant-mediated scaffolding of peptized pseudoboehmite nanoparticles, Langmuir vol. 26 (12) (2010) 10063–10067.
[25] S. Nazari, G. Karimi, E. Ghaderi, K. Mansouri Moradian, Z. Bagherpor, Synthesis and characterization of γ-alumina porous nanoparticles from sodium aluminate liquor with two different surfactants, Int. J. Nanosci. Nanotechnol. vol. 12 (4) (2016) 207–214.
[26] F.G. Torres, G.E. De-la-Torre, Synthesis, characteristics, and applications of modified starch nanoparticles: A review, Int. J. Biol. Macromol. vol. 194 (2022) 289–305, https://doi.org/10.1016/j.ijbiomac.2021.11.187.
[27] F. Li, Y. Wang, X. Gao, Y. Wang, Preparation of high pore volume γ-Al2O3 nanorods via 'gibbsite-AACH' precursor route in a membrane dispersion microreactor, Microporous Mesoporous Mater. (2022), 111680.
[28] B. Xu, J. Long, H. Tian, Y. Zhu, X. Sun, Synthesis and characterization of mesoporous γ-alumina templated by saccharide molecules, Catal. Today vol. 147 (2009) S46–S50.
[29] D.F. Niero, O.R.K. Montedo, A.M. Bernardin, Synthesis and characterization of nano α-alumina by an inorganic sol–gel method, Mater. Sci. Eng. B vol. 280 (2022), 115690.

[30] W. Ojok, J.P. Bolender, J. Wasswa, E. Ntambi, W. Wanasolo, B. Moodley, Facile synthesis and characterization of multi-walled carbon nanotubes decorated with hydroxyapatite from cattle horns for adsorptive removal of fluoride, Heliyon vol. 9 (3) (2023), e14341, https://doi.org/10.1016/j.heliyon.2023.e14341.
[31] S. Raghav, D. Kumar, Comparative kinetics and thermodynamic studies of fluoride adsorption by two novel synthesized biopolymer composites, Carbohydr. Polym. vol. 203 (2019) 430–440.
[32] M.J. Temkin and V. Pyzhev, Recent modifications to Langmuir isotherms, 1940.
[33] H.M.F. Freundlich, Over the adsorption in solution, J. Phys. Chem. vol. 57 (385471) (1906) 1100–1107.
[34] R. Kumari, A. Kumar, S. Basu, Aluminium fumarate-based polymer matrix composite for selective removal of fluoride from groundwater, Environ. Nanotechnol., Monit. Manag. vol. 17 (November 2021) (2022), 100642, https://doi.org/10.1016/j.enmm.2022.100642.
[35] I. Langmuir, The adsorption of gases on plane surfaces of glass, mica and platinum, J. Am. Chem. Soc. vol. 40 (9) (1918) 1361–1403.
[36] B. Barik, P.S. Nayak, L.S.K. Achary, A. Kumar, P. Dash, Synthesis of alumina-based cross-linked chitosan–HPMC biocomposite film: an efficient and user-friendly adsorbent for multipurpose water purification, N. J. Chem. vol. 44 (2) (2020) 322–337.
[37] D. Kang, X. Yu, M. Ge, M. Lin, X. Yang, Y. Jing, Insights into adsorption mechanism for fluoride on cactus-like amorphous alumina oxide microspheres, Chem. Eng. J. vol. 345 (February) (2018) 252–259, https://doi.org/10.1016/j.cej.2018.03.174.
[38] W. Li, C.-Y. Cao, L.-Y. Wu, M.-F. Ge, W.-G. Song, Superb fluoride and arsenic removal performance of highly ordered mesoporous aluminas, J. Hazard. Mater. vol. 198 (2011) 143–150.
[39] S. Jagtap, M.K.N. Yenkie, N. Labhsetwar, S. Rayalu, Defluoridation of drinking water using chitosan based mesoporous alumina, Microporous Mesoporous Mater. vol. 142 (2–3) (2011) 454–463.
[40] N. Mahfoudhi, S. Boufi, Porous material from cellulose nanofibrils coated with aluminum hydroxyde as an effective adsorbent for fluoride, J. Environ. Chem. Eng. vol. 8 (3) (2020), 103779.
[41] A. Jeyaseelan, M. Naushad, T. Ahamad, N. Viswanathan, Design and development of amine functionalized iron based metal organic frameworks for selective fluoride removal from water environment, J. Environ. Chem. Eng. (2020), 104563.
[42] Y.S. Ho, J.C.Y. Ng, G. Mckay, Kinetics of pollutant sorption by biosorbents: review, Sep. Purif. Methods vol. 29 (2) (2000) 189–232.
[43] W.J. Weber, J.C. Morris, Kinetics of adsorption on carbon from solution, J. Sanit. Eng. Div. vol. 89 (2) (1963) 31–60.
[44] V. Kimambo, et al., Optimization of fluoride removal using calcined bauxite: Adsorption isotherms and kinetics, Groundw. Sustain. Dev. vol. 21 (2023), 100922.
[45] M. Eissen, Sustainable production of chemicals–an educational perspective, Chem. Educ. Res. Pract. vol. 13 (2) (2012) 103–111.
[46] M.-J. Kim, S.-H. Hong, J.-I. Lee, C.-G. Lee, S.-J. Park, Removal of fluoride from water using thermally treated dolomite and optimization of experimental conditions using response surface methodology, Desalin. Water Treat. vol. 155 (2019) 311–320.
[47] M. Egor, et al., Cellulosic ternary nanocomposite for affordable and sustainable fluoride removal, ACS Sustain. Chem. Eng. vol. 9 (38) (2021) 12788–12799.
[48] R.A. Sheldon, Metrics of green chemistry and sustainability: past, present, and future, ACS Sustain. Chem. Eng. vol. 6 (1) (2018) 32–48.